Light Scattering and Proposed Baffle Configuration for the LIGO

Second Draft, 11 January 1989

*Kip S. Thorne**

California Institute of Technology, Pasadena, California 91125

ABSTRACT

When light, hitting a mirror, scatters out of the main beam of an interferometric gravitational-wave detector, then makes its way back into the beam via reflection, scattering, and/or diffraction off the LIGO vacuum pipe, baffles, or mirrors, it produces a slight phase shift in the main beam's light. Wiggle of the main beam and vibrations of the vacuum pipe and baffles cause this phase shift to oscillate, simulating a gravitational wave. The dominant contributions to this gravitational-wave noise are here computed; and those computations are used to suggest constraints on the design of the baffles for the LIGO. If these constraints are followed, there is no reason to expect serious problems with light scattering in the LIGO, even in very advanced detectors of the highest currently projected sensitivities. By contrast, without baffles there would be severe and perhaps insurmountable light-scattering noise.

Contents

Supported in part by the National Science Foundation Grants AST-8514911 and PHY-8803557

I. Overview

This document is divided into three main sections: Section II presents the recommended constraints on baffle design that come out of the scattering calculations. Section III presents the results of the scattering calculations: the spectral density $\tilde{h}^2(f)$ of the gravitational-wave noise due to the dominant scattering processes, and a set of simple formulae that can be used to compute scattering noise from these and other processes. Section IV sketches the details of the scattering calculations.

II. Recommended Constraints on Baffle Design and Other LIGO Features.

1. Baffle Spacing and Height

The most severe scattering noise in the absence of baffles comes from light that leaves one mirror and travels down the vacuum pipe, reflecting many times off the pipe walls, until it reaches the other mirror. It is essential that the baffles stop all such light.

The larger the angle θ that a light ray makes to the pipe's central axis, the greater the number of reflections it will undergo in traveling from one end of the pipe to the other, and the greater will be the power lost from the ray to scattering and absorption at each reflection. Correspondingly, there is a maximum angle θ_o such that for $\theta > \theta_o$ light is strongly attenuated in traveling from one end of the pipe to the other, while for $\theta < \theta_o$ it is weakly attenuated. The turn on of attenuation as θ increases through θ_o is very sharp; see Eq. (2.3) below. The baffles must be designed to stop (almost) all light with angles $\theta < \theta_o$; light with $\theta > \theta_o$ will get adequately attenuated without the help of baffles. If the pipe is corrugated, then θ_o will be approximately equal to the "Rayleigh angle" below which the tops of the corrugations look like an excellent mirror:

$$\theta_o \sim \theta_R = \left(\frac{2\lambda}{a}\right)^{1/2} = 0.6\times10^{-2}\left(\frac{\lambda}{0.4\,\mu\text{m}}\right)^{1/2}\left(\frac{1.5\,\text{cm}}{a}\right)^{1/2} . \qquad (2.1)$$

Here λ is the wavelength of light used, $2\pi a$ is the wavelength of the corrugations, and it is assumed that the corrugations have an amplitude (half the peak-to-trough distance) of a. If the pipe is not corrugated, then θ_o will be somewhat larger than (2.1). Rai Weiss (private communication) shows that for stainless steel and for the least attenuated polarization component of the light, and for angles $\theta \ll \pi/2$, the fraction of the photons lost in each bounce is $0.55\,\theta$ and correspondingly, the fraction that survive is $1-0.55\,\theta$. Since the total number of reflections in going from one end of the pipe to the other is no less than $L\,\theta/2R$ where L is the length of the pipe and R is its radius, the fraction of the photons that survive the entire trip is

$$(1-0.55\,\theta)^{L\,\theta/2R} \cong \exp\left(-\frac{L\theta^2}{3.6\,R}\right) , \qquad (2.2)$$

which cuts off very sharply at

$$\theta_o = 4\sqrt{3.6\,R/L} = 0.1 . \qquad (2.3)$$

For $\theta = 0.1$ the attenuation is 10^8 in energy (10^4 in amplitude, which is the relevant thing for scattering noise $\tilde{h}$); for $\theta = 0.05$ the attenuation is only 10^2 in energy (10 in amplitude). For further details see a forthcoming report by Weiss. It will be important in the design of the baffles to have a fairly accurate estimate of θ_o. Such an estimate and methods of minimizing θ_o are being developed by Weiss.

These considerations, together with a calculation of the dominant scattering noise effects in the presence of baffles (Secs. III.C and IV.C below) produce the following recommendation for constraints on the heights and spacings of the baffles:

Recommendation 1. Consider any point at the end of the pipe, at which the center of a mirror might be

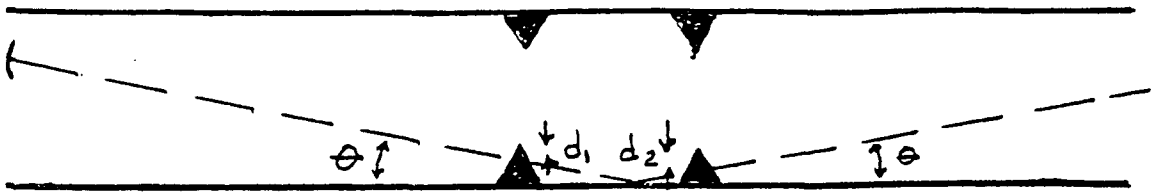

Fig. 2.1. The encounter of a ray that has angle θ with a pair of baffles. The distances d_1 and d_2 must satisfy $d_1+d_2 \geq 12\delta H$.

placed. Consider any straight ray eminating from that point in any direction that makes an angle $\theta < \theta_o$ with the pipe's central axis (Fig. 2.1). Follow that ray down the pipe, letting it penetrate straight through any baffles it encounters and reflecting it specularly off the wall at each wall encounter. The baffles must be so designed that the ray at least twice — once near the first end of the pipe and once near the second end — encounters a pair of baffles in the manner of Fig. 2.1; and in each of these encounters the points at which the ray penetrates the baffles must be at distances d_1 and d_2 below the baffle tops such that $d_1+d_2 \geq 2\delta H$. Here δH is a *height safety factor* that appears in the diffraction calculations. Those calculations suggest that $\delta H = 1$ cm is a reasonable value. Of course, rays that never encounter the pipe are not subject to the above constraint; and rays that encounter it only once are required to have only one encounter of the type shown in Fig. 2.1. No baffles should be closer to any detector mirror than 10 meters. [*Note*: The requirement for two encounters of the type of Fig. 2.1, one near each end of the pipe, requires for its implementation twice as many baffles as would be needed if one such encounter were sufficient. If the cost of the baffles is inordinately high we could consider relaxing the requirement back to one such encounter, and insist that it occur near the corner mirror. For a discussion of the dangers inherent in such a decision, see Sec. III.C.]

The following is a suggestion of how to implement this recommendation; see Fig. 2.2: Begin at the plane of the corner mirror and move into the vacuum pipe some (arbitrary) small distance l_1 — but a distance of at least 10 meters and at least as large as (the closest an interferometer beam is likely to come to the pipe wall)$/\theta_o$. At this location place the first baffle. Thereafter, for a distance $2R/\theta_o$ down the pipe place baffles with heights and spacings governed by the following law: If H_n is the height of baffle n and s_n is the spacing between baffles n and $n+1$, then

$$H_{n+1}+H_n \geq \theta_o s_n + 2\delta H \ . \tag{2.4a}$$

(Provision is made here for the possibility that one might want to vary the baffles' spacings so as to put the baffles at particularly convenient locations, and correspondingly one might want to vary the baffle height.) This first series of baffles, which terminates after a distance $2R/\theta_o$, is designed to intercept in the manner of Fig. 2.1 all rays with $\theta = \theta_o$. Thereafter, moving on down the pipe, the baffle spacing can gradually increase: Baffle n at a distance d_n from the first baffle, and baffle $n+1$ at $d_{n+1} = l_n + s_n$ must have heights and separations given by

$$H_n+H_{n+1} \geq \frac{s_n}{d_n} 2R + 2\delta H \ . \tag{2.4b}$$

Once the middle of the pipe has been reached, this sequence of baffles stops. Then, if the requirement is

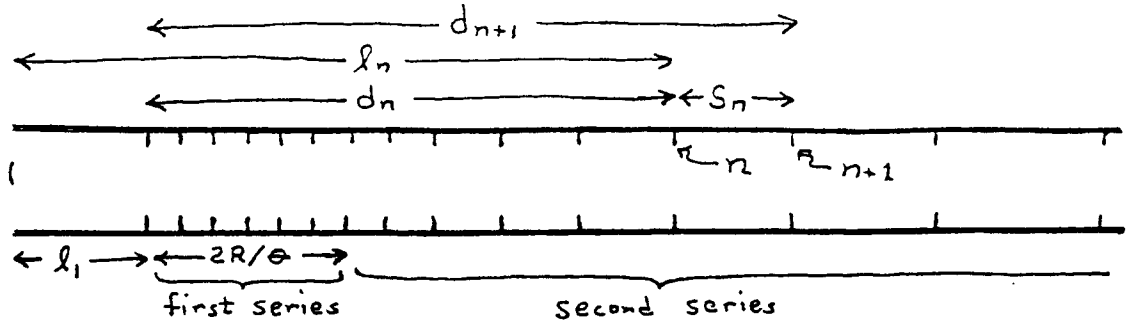

Fig. 2.2 A possible implementation of Recommendation 1 on baffle heights and spacings.

relaxed to only one encounter of the type of Fig. 2.1, no baffles are needed in the outer half of the pipe. If, however, the recommendation of two such encounters is followed, then one must begin once more at the outer end of the pipe and build two sequences of baffles in the same manner as above [Eq. (2.4a) for a distance $2R$, then (2.4b) to pipe's middle].

The total number of baffles in this implementation is readily shown to be, if baffles are put in both ends of the pipe as recommended,

$$N_b = \frac{2R}{H-\delta H}\left[1+\ln\left[\frac{L\theta_o}{4R}\right]\right], \tag{2.5}$$

where H is the mean baffle height and δH is the height safety factor. For a smooth pipe with $\theta_o = 0.1$ this formula gives $N_b \simeq 146[5\text{ cm}/(H-\delta H)]$. For a corrugated pipe with $\theta_o = 0.01$ it gives $N_b \simeq 90[5\text{ cm}/(H-\delta H)]$. If we are willing to live dangerously and baffle only the inner half of the pipe, the number of baffles is reduced to $N_b \simeq 73[5\text{ cm}/(H-\delta H)]$ for a smooth pipe and $N_b \simeq 45[5\text{ cm}/(H-\delta H)]$ for a corrugated pipe.

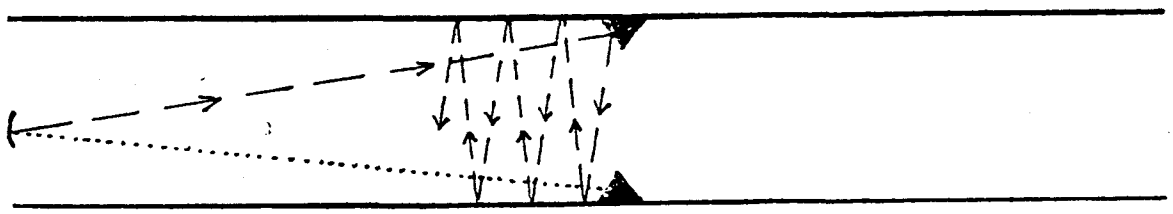

Fig. 2.3 Because of their 45-degree inclination, the baffle faces reflect light into transverse directions (long-dashed lines), where in a sequence of bounces off the vacuum pipe walls most of it gets absorbed. The probability $dP/d\Omega$ for light to be scattered off the baffle and back to the mirror from which it came (dotted lines) should be made as small as possible, without undue cost, by appropriate choice of the baffle material and surfacing.

2. Shape and Reflectivity of the Faces of the Baffles.

The faces of the baffles should be highly reflecting and should be inclined at an angle of about 45 degrees to the vacuum pipe wall. This will enable them to reflect most of the scattered light into transverse directions, thereby preventing it from subsequently reaching either mirror, except by one or more scatterings: see Fig. 2.3. Stated more precisely:

Recommendation 2. (i) The scattering probability $dP/d\Omega \equiv d\sigma/d\Omega dA$ is defined to be the cross section $d\sigma$ for a unit area dA of baffle to scatter light into a unit solid angle $d\Omega$. This scattering probability

should be made as small as possible, without undue expense, for light that comes in from a mirror (hitting the baffle surface at 45 degrees to its normal), and is scattered back toward that same mirror. (ii) The baffle shape and tolerances on its shape should be chosen to guarantee that the total amount of light that is reflected (specularly) off the baffle and that subsequently makes its way back to the mirror by any route whatsoever (e.g., via the dashed lines of Fig. 2.4) is less than the amount that is scattered directly off the baffle and back to the mirror (dotted lines in Fig. 2.3). [*Note*: This is especially important for baffles near the ends of the pipe, and less so for baffles farther from the ends; see the discussion of baffle scattering in Sec. III.D.]

This probably will not be difficult to achieve. It will constrain, for example, the sharpness of the baffle edges and the precise angle of the baffle faces to the vacuum wall (e.g. 45.5 degrees versus 46 degrees) and tolerances on that angle.

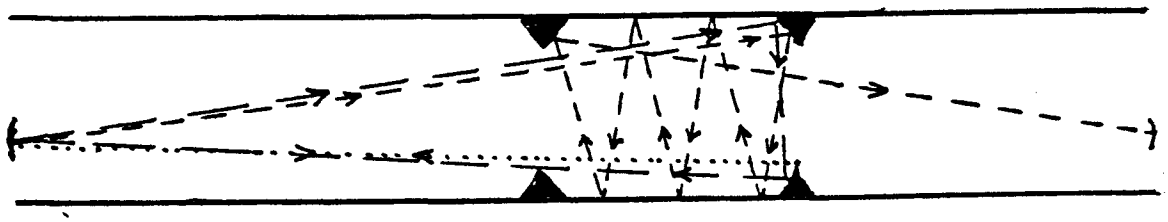

Fig. 2.4 Several routes by which light that reflects (rather than scatters) off a baffle can subsequently make its way back to a mirror. The baffle shape and tolerances should be specified so as to guarantee that the total amount of light that gets back to the mirrors by such routes is less than the amount that is scattered directly back from the baffles (dotted route in Fig. 2.3).

3. Shape of the baffle edges.

Cadez, Saulson, Weiss, and I have discussed at various times the desirability of making the edges of the baffles jagged, i.e. giving them quasi-random variations in height with amplitudes of a few millimeters and wavelengths as short as is convenient. The purpose of this jaggedness is to randomize the phase of light that diffracts off the baffle edge, thereby lessening the gravitational-wave noise that results from such light. It turns out that jaggedness has a significant beneficial effect only in the case of mirrors that are within a distance $\sqrt{\lambda L} = 4\,\text{cm}$ of the center of the pipe's cross section (see Sec. IV.E for details); and even then the randomness of phases introduced by irregularities in the mirrors, the photodiode, and the shape of the vacuum pipe might be sufficient to protect adequately against coherent effects without the additional help of jaggedness. However, it is not certain that this is the case. Therefore, I am led to the following recommendation:

Recommendation 3. I recommend that the edges of the baffles be made jagged rather than smooth. The jaggedness should consist of height variations with rms peak-to-peak amplitudes

$$\Delta H \geq \frac{\lambda L}{2R} = 2\,\text{mm}\left[\frac{\lambda}{1.2\,\mu\text{m}}\,\frac{L}{4\,\text{km}}\,\frac{60\,\text{cm}}{R}\right] . \tag{2.6}$$

Here λ is the longest wavelength of light expected to be used in the LIGO. The height variations can be random or regular; it does not matter which. What is important is (i) that they have the shortest wavelength that can be achieved without great effort, preferably $\ll 1$ cm; and (ii) that they contain as little longer wavelength component as can be achieved without great effort. [*Note*: If future calculations

suggest that one should worry about phase coherence for mirrors far from the center of the pipe, as well for those close to the center, then to protect against it the rms amplitude ΔH of height variations should be 3 times larger than (2.6).]

4. Straightness and Roundness of the vacuum pipe.

It is *not* desirable for the pipe to be perfectly straight and round. The reason is that for a straight, round pipe and for mirrors near the pipe's center, light that scatters off one mirror and then propagates to the other mirror via an even number of reflections off the pipe wall will get focused and amplified in the reflections by a net factor that can be as large as $2R/\sqrt{\lambda L} = 30$ in amplitude (1000 in energy). To prevent this, there must be fluctuations in the straightness at least, and if convenient also in the roundness (Sec. IV.B). On the other hand, if the fluctuations are too great, then they will amplify certain types of scattering noise (Sec. III.C). This leads to the following recommendation:

Recommendation 4. A "longitudinal curve" on the vacuum pipe's wall is defined to be the intersection of that wall with any plane containing the straight central axis of the pipe. At any point on the wall, define the angle μ_o to be the angle between the longitudinal curve through that point and the central axis of the pipe. Then there should be fluctuations in μ_o with rms amplitude σ_{μ_o} in the range

$$10^{-4} \text{ radians} < \sigma_{\mu_o} < 10^{-3} \text{ radians} . \tag{2.7a}$$

Accompanying these angular fluctuations there should be fluctuating linear offsets ξ_o of the pipe's central axis with rms amplitude

$$\sigma_{\xi_o} \geq 1 \text{ cm} . \tag{2.7b}$$

For detailed justifications of these limits see Secs. III.C, IV.B, and IV.E.

5. Beam Wiggle.

In the design and development of detectors for the LIGO, account should be taken of the effect of beam wiggle on scattering. This might be the most serious factor constraining the allowable beam wiggle — especially if only one end of the pipe is baffled rather than both ends. For details see the paragraph following Eqs. (3.25).

6. Computer Simulations of Scattering

I am not sufficiently confident of my scattering calculations to justify basing the final LIGO baffle design solely on them.

Recommendation 5. I recommend that computer simulations be carried out to check my calculations.

7. Parameters of Final Baffle Design

Recommendation 6. The parameters of the final baffle design should be so chosen as to keep smaller than about 1/10 the standard quantum limit (3.2) the noise levels (3.25)—(3.33) — at least in the case where a mode cleaner is used on the interferometer output, and if possible also without a mode cleaner. If the general design of the baffles differs from that recommended here, then for the chosen design the noise levels for the processes in Secs. III.B—III.E should be recomputed, and the design should be adjusted to keep them below about 1/10 of (3.2).

III. Results of Scattering Calculations

The formulas for scattering noise in this section are probably accurate to within a factor 10 and perhaps better. This seems accurate enough for our purposes — and higher accuracy would require far more effort than I have expended. In most of the formulas factors of order unity (2's, π's, etc. have been kept because they occasionally combine to give a net multiplicative factor of order 10 or larger. However, the precise combinations of 2's, π's, etc. that are quoted are almost certainly not correct.

The formulas are given for Fabry-Perot interferometers. I have not analyzed scattering noise in Michelson interferometers in detail, except for an old (May 1987) calculation of one rather unimportant scattering process. It would be worthwhile for somebody to extend this report's analysis to Michelsons.

The parameters that will appear in the scattering formulas are listed here in alphabetical order for ease of reference:

B — effective number of bounces that the light beam makes in the arms of the interferometer; defined more precisely by the equation preceding (3.7) below; for a simple interferometer or a light-recycled interferometer optimized to gravitational waves with frequency f, this quantity is (see page 424 of Ref. 5)

$$B = \frac{c}{2\pi f L} = \frac{4\times 10^3}{f/10\,\mathrm{Hz}} . \tag{3.1}$$

We shall use this value in our numerical estimates. For an interferometer with resonant recycling B can be larger than this. Using that larger B would produce smaller levels $\tilde{h}(f)$ of scattering noise than those quoted in this report.

d_n — distance of baffle n from the first baffle at the end of the pipe nearest to baffle n; approximately equal to the smaller of l_n and $L-l_n$.

$\frac{d\sigma}{dx\,d\theta'}$ — the differential cross section for diffracting light off a baffle, either in the case of ordinary diffraction or the case of diffraction-aided reflection; see Eq. (3.9) for the precise definition of this cross section; see Eqs. (3.10) and (3.15) & (3.16) for formulas for the cross section.

$\frac{d\sigma}{dx}$ — the total cross section for diffracting light off a baffle into angles larger than the incoming angle. See Eqs. (3.11) and (3.17) for formulas in the case of ordinary diffraction and diffraction-aided reflection, respectively.

$\frac{d\sigma}{d\Omega dA}$ — the scattering probability for the baffle surfaces, i.e. the cross section $d\sigma$ for a unit area dA of baffle surface to scatter light into a unit solid angle $d\Omega$. In this report this scattering probability is used only for incoming and outgoing light parallel to each other and at an angle of about 45 degrees to the baffle surface. For numerical estimates we use the conservative value 0.1 for this scattering probability.

f — the frequency of modulation of scattered light produced by its encounters with baffles and pipe walls.

$\tilde{h}(f)$ — square root of spectral density of noise in gravitational-wave units, i.e. $\tilde{h}(f) = \sqrt{S_h(f)}$ in the notation of Reference 5; units are "strain per root Hertz".

$\hbar = 1.054\times 10^{-27}$ erg sec — Planck's constant divided by 2π.

H — the mean height of the baffles' tops above the inner face of the vacuum pipe; for numerical estimates we use $H = 6$ cm.

H_n — the height of baffle n; in numerical estimates we shall use $H_n = H = 6$ cm.

δH — "height safety factor": the minimum height that a baffle should be above that required to intercept rays from mirrors; see Eqs. (2.4); the value suggested in this document is $\delta H = 1$ cm, and this is assumed in all numerical estimates.

ΔH — the maximum peak-to-valley variations of height of the baffles ("jaggedness"); assumed equal to 6 mm in numerical estimates, see Eq. (2.2)

l_n — the distance of baffle n from the closest interferometer mirror.

l_{Rn} — the "reduced distance" of a baffle pair, n and $n+1$, from the mirrors; given by $l_{Rn} \equiv l_n(L-l_{n+1})/L$ [where baffle n is presumed to be closer to the nearest mirror than baffle $n+1$]..

L — the length of an arm of the interferometer; assumed equal to 4 km in numerical estimates.

m — the mass of a mirror, assumed equal to 1000 kg in the numerical evaluation of quantum noise [Eq. (3.2) below].

N_b — the total number of baffles; see Eq. (2.5).

$P_{sc}(\theta)$ "scattering probability": the probability that a photon from the main beam gets scattered into a unit solid angle about a direction that makes an angle θ with the main beam. In this report it is assumed that $P_{sc}(\theta) = \alpha/\theta^2$, where $\alpha = 10^{-6}$.

$P_{rec}(\theta)$ — "recombination probability": the probability that a previously scattered photon impinging on a mirror at an angle θ to the mirror's normal will recombine with the main beam in such a way as to contribute to the scattering noise $\tilde{h}(f)$. This P_{rec} depends on whether a mode cleaner is used on the interferometer output. With a mode cleaner, P_{rec} is given by Eq. (3.5); without, by Eq. (3.6).

R — the radius of the vacuum pipe; assumed equal to 60 cm in numerical estimates.

Y_o — the distance from the center of the main beam to the mean position (smoothed over jaggedness) of the nearest baffle edge; assumed equal to 20 cm in numerical estimates when a small Y_o is the most dangerous.

s_n — the spacing between baffles n and $n+1$; assumed in numerical estimates to be given by Eqs. (2.4) with $R = 60$ cm, $H_n = 6$ cm for all n and $\delta H = 1$ cm; i.e. $s_n = 10\,\text{cm}/\theta_o$ for the first $120\,\text{cm}/\theta_o$ length of baffles near each end; thereafter $s_n = d_n/12$.

α — coefficient that appears in the approximate formula $P_{sc}(\theta) \equiv dP/d\Omega = \alpha/\theta^2$ [Eq. (3.4)] for the scattering of main-beam light off the interferometer's mirrors. In this formula $P_{sc}(\theta) = dP/d\Omega$ is the probability that a photon in the main beam will be scattered into a unit solid angle around a direction that makes an angle θ with the normal to the mirror. In numerical estimates we shall use a value $\alpha = 10^{-6}$ appropriate to supermirrors [Sec. III.A.1].

λ — the wavelength of light used in the interferometer; for numerical estimates we shall set $\lambda = 0.4\,\mu$m.

$\bar{\eta}$ — the photodiode efficiency, averaged over the spot made by the main beam on the photodiode: assumed equal to 0.9 in numerical estimates.

$\bar{\mu}$ — the value of an angle μ averaged over times long compared to the gravitational-wave period. This μ is defined as follows: A "longitudinal curve" on the vacuum pipe's inner wall is the intersection of that wall with any plane containing the central axis of the pipe. Consider a typical point at which light reflects off the vacuum pipe's inner wall. Then μ is the angle between the longitudinal curve at that typical reflection point and the line-of-sight direction between the two points where the reflecting ray originates and terminates. (Those origination and termination points are either on the mirrors or on the edges of diffracting baffles.) We sometimes shall refer to μ as the "slope" of the wall, and sometimes as its "angle".

$\tilde{\mu}(f)$ — the square root of the spectral density of fluctuations $\delta\mu(t)$ in the angle μ defined above. These fluctuations are due to (seismic-induced) acoustic oscillations of the vacuum pipe wall, plus — if only one end of the vacuum pipe or neither end is baffled — wiggle of the main beam; see the paragraph following Eqs. (3.25). We shall assume, for numerical estimates, that $\tilde{\mu}(f) = 10^{-10}\,\mathrm{Hz}^{-1/2}\times(10\,\mathrm{Hz}/f)$; see the passages following Eq. (3.22) for discussion of the reasons behind this value.

μ_o — the angle between a longitudinal curve on the vacuum pipe's inner wall and the straight-line central axis of the pipe.

σ_{μ_o} — rms value of the angle μ_o

σ_{ξ_o} — rms value of the lateral offset ξ_o of the pipe's central axis. This lateral offset, like μ_o, is produced by (desirable) crookedness in the way the pipe is laid during construction. For numerical estimates we shall use $\sigma_{\xi_o} = 1$ cm.

σ_H — the maximum wavelength of the jaggedness of the baffles, i.e. the wavelength above which the spectral density of the jaggedness is small.

σ_M — the mean wavelength for variations in the phase of scattered light along the edges of the baffles — variations produced by irregularities in the scattering mirrors; see Eq. (4.5d) and associated discussion

σ_{pd} — the mean wavelength for photodiode-irregularity-induced variations in phase along the edges of the baffles; see Eq. (4.11) and associated discussion.

$\tilde{\xi}(f)$ — the square root of the spectral density of fluctuational displacements of a typical point on a typical baffle — either longitudinal displacements or radial displacements. For numerical estimates we shall assume that the baffles are sufficiently well anchored that they experience displacements only of order the seismic noise; i.e. we shall assume $\tilde{\xi}(f) = 10^{-7}\,\mathrm{cm\,Hz}^{-1/2}\times(10\,\mathrm{Hz}/f)^2$, corresponding to the level of seismic noise at the likely LIGO sites.

θ — the angle between a ray of scattered light and the central axis of the main beam.

θ' — the angle (value of θ) into which light diffracts when it encounters a baffle.

θ_n — the minimum value of θ that a ray must have, when encountering baffles n and $n+1$, in order to avoid being caught by them; given by Eq. (3.13).

This section III is organized as follows: Sec. III.A presents a set of simple formulas which can be used to compute the noise due to a wide variety of scattering processes (scattering of the main beam off a mirror, diffraction of scattered light off baffles, reflection of scattered light off the pipe walls, recombination of scattered light with the main beam, ...). These formulas underlie most of the noise formulas of this report, and they can be used for other, future noise calculations. The need for baffles is elucidated in Section III.B by discussing the dominant scattering noise effect for a LIGO without baffles: scattering off a mirror, followed by reflections off the vacuum pipe wall, propagation to the other mirror, and recombination there with the main beam. The remaining sections discuss what appear to be the dominant scattering noise effects in the presence of baffles: scattering off one mirror, followed by a diffraction-aided reflection between a pair of baffles, followed by a series of reflections off the pipe wall and possibly a second diffraction-aided reflection, followed by recombination with the main beam at the second mirror (Sec. III.C); scattering off a mirror, followed by scattering off the baffles, propagation back to the mirror and recombination there with the main beam (Sec. III.D).

In discussing these scattering processes we shall need to compare their noise levels with the best sensitivities that are hoped for in the LIGO. As a measure of the best sensitivities we shall use the standard

quantum limit

$$\tilde{h} = \left[\frac{8\hbar}{m(2\pi f L)^2}\right]^{1/2} = \frac{4\times10^{-24}}{\sqrt{\text{Hz}}}\,\frac{10\,\text{Hz}}{f} \tag{3.2}$$

[Eq. (121) of Ref. 5]. We shall regard scattering noise as acceptably small if it is at least one order of magnitude below this level. (The one-order-of-magnitude safety factor is to allow for inaccuracies in the scattering calculations.)

A. Formulas for Use in Intensity Analyses of Scattering

It is argued in various places in this document [see especially the summary and analysis in Sec. IV.E, the paragraph following Eq. (4.11), and Sec. IV.A.5] that by the time scattered light reaches the mirror or photodiode at which it will recombine with the interferometer's main beam to produce noise, the phases of light coming from different directions will be so scrambled that coherent superposition is relatively unimportant. As a result, computations of the noise due to scattered light can be carried out using intensity techniques in which the precise phase of any bit of light is ignored. In this section I give a number of useful formulas for such calculations; these formulas are derived in Sec. IV.A

1. Scattering Probability $P_{sc}(\theta)$

When the main beam of the interferometer hits a mirror, irregularities in the mirror scatter a bit of the main-beam light. We shall denote by $P_{sc}(\theta)$ the probability that a main-beam photon will get scattered into a unit solid angle in a direction that makes an angle θ with the specularly reflected main beam,

$$P_{sc} = \frac{d\,\text{Probability}}{d\Omega}\,. \tag{3.3}$$

The angles relevant to the LIGO are $\theta_o \gtrsim \theta \gtrsim 2Y_o/L$; i.e. 0.1 or 0.01 radians to 10^{-4} radians; i.e. 5 degrees or 30 minutes down to 0.3 minutes of arc. The most relevant scattering data I know of are: (i) measurements with a poor quality mirror by Michelle Stephens[1] in the range $0.011 \le \theta \le 0.027$, which are well fit by $P_{sc} \simeq 2.4\times10^{-3}(1-\mathcal{R})/\theta^2$, where $\mathcal{R} = 0.988$ is the reflectivity of the mirror that she used; and (ii) measurements on supermirrors in the range $XXX \le \theta \le XXX$ by Elson and Bennett[2], which are well fit by[3] $P_{sc}(\theta) = 1.5\times10^{-6}/\theta^2$. Assuming that P_{sc} is proportional to $1-\mathcal{R}$, there is reasonable agreement between Stephens' results and those of Elson and Bennett. Note, further, that the dependence on θ, $P_{sc} = \alpha/\theta^2$ with $\alpha \sim 10^{-6}$, puts equal amounts of power into equal increments of $\ln\theta$, and it leads to a total probability for scattering photons out of the main beam given by $P_{\text{total}} = \int P_{sc} 2\pi\sin\theta d\theta \simeq 2\pi\alpha\ln(\sqrt{L/\lambda}) = 7\times10^{-5}(\alpha/10^{-6})$. This is so close to the total losses of supermirrors ($\simeq 10^{-4}$) that there is no room for excess scattering, beyond that of the formula $P_{sc} = \alpha/\theta^2$, for angles θ below those at which the scattering has been measured. Thus, it seems reasonable to assume (and we shall do so throughout this report) that not only in the measured region but also down to the LIGO's smallest angles, which are 30 times smaller, the scattering probability is given by

$$P_{sc} = \frac{\alpha}{\theta^2}\,, \quad \text{with } \alpha = 10^{-6}\,. \tag{3.4}$$

The relationship of this scattering probability to the mirror's irregularities, and the spatial dependence of the phase of the scattered light are discussed in Sec. IV.A.2.

2.Probability $P_{rec}(\theta)$ for Recombination of Scattered Light with the Main Beam

After leaving the main beam, scattered light can interact with the walls of the vacuum pipe and with the baffles in a variety of ways to be discussed below, and then some of the scattered light can recombine with the main beam in two ways: By hitting a mirror and there scattering back into the main beam, or by hitting the corner mirror and being transmitted through it, along with the main beam, onto the photodiode. We shall consider these two recombination processes in turn.

Scattering back into main beam. When a scattered photon impinges on the mirror at an angle θ to the incoming main beam, it has a probability $P_{sc}(\theta) = \alpha/\theta^2$ of being scattered into a unit solid angle in the direction of the reflected main beam. In order to actually rejoin the main beam rather than going into some other mode of the Fabry-Perot cavity, the photon must scatter into a solid angle which is equal to that subtended by the main beam's spot on the distant mirror, $\Delta\Omega = \lambda L/L^2 = \lambda/L$. Correspondingly, the probability for the photon to recombine with the main beam via scattering is

$$P_{rec}(\theta) = \frac{\alpha}{\theta^2}\left[\frac{\lambda}{L}\right] . \tag{3.5}$$

Transmission through mirror onto photodiode. Scattered light, arriving at the photodiode from a direction that makes an angle θ with the main beam, has its phase fronts at an angle θ relative to those of the main beam. Since the phase fronts of the main beam and the beam from the other arm of the detector have been made to agree at the photodiode, so far as possible, this means that the scattered light's phase fronts disagree in angle by θ with those of the light from the other arm. The result is a pattern of interference fringes on the photodiode with wavelength λ/θ. In these fringes the scattered light alternately increases, then decreases the light intensity and hence the photocurrent. If the photodiode's efficiency η for converting light intensity into photocurrent were spatially uniform, these fringes would give a net averaged contribution to the photocurrent that is the Fourier transform (at wave number $\theta k = 2\pi\theta/\lambda$) of the Gaussian shape (4.1) of the main beam — and because Fourier transforms of Gaussians are Gaussians and are notoriously small out on the wings where we are operating ($\sim e^{-(\pi/4)[\theta/\sqrt{\lambda/L}]^2}$), the effects of the scattered light would be totally negligible. Unfortunately, the efficiency η will be spatially variable due to imperfections in the photodiode; and correspondingly the effect of the scattered light on the photocurrent will be proportional to a spatial Fourier transform of the photodiode efficiency.

More specifically (see Sec. IV.A.3), if the scattered light's effect is described by the probability $P_{rec}(\theta)$ for each scattered photon to recombine at the photodiode with the main beam in such a way as to act like a main-beam photon, then that $P_{rec}(\theta)$ will be essentially the square of the spatial Fourier transform of η. A conservative estimate of the magnitude of that Fourier transform (more likely an overestimate than an underestimate; see Sec. IV.A.3 for details) gives

$$P_{rec} = \frac{(1-\bar{\eta})^2}{2\theta}\left[\frac{\lambda}{L}\right]^{1/2} . \tag{3.6}$$

Here $\bar{\eta}$ is the spatially averaged efficiency of the photodiode, which in numerical estimates we shall take equal to 0.9.

Comparison of recombination via scattering with recombination via transmission to photodiode. The probability (3.6) for recombination via transmission to the photodiode is always (for all relevant θ) several orders of magnitude larger than the probability (3.5) for recombination via scattering. Fortunately, if recombination via transmission becomes a serious noise source, it can be suppressed by putting a mode cleaner on the output of the interferometer. Thus, with a mode cleaner recombination by scattering dominates: without a mode cleaner recombination by transmission to the photodiode dominates.

3. Scattering Noise Expressed as $\tilde{h}(f)$

When scattered light recombines with the main beam, it produces a change of phase $\delta\Phi_{mb}$ in the main beam. This $\delta\Phi_{mb}$ fluctuates slightly due to fluctuations in the phase of the scattered light — fluctuations put onto the scattered light by interactions with the pipe walls and baffles. The square root of the spectral density of those phase fluctuations is given by

$$\tilde{\Phi}_{mb}(f) = \cos(\Phi_{sc}-\Phi_{mb})\left[\frac{dE_{sc}/dtdf}{I}\right]^{1/2} .$$

Here $\Phi_{sc}-\Phi_{mb}$ is the phase difference between the scattered light and the main beam, I is the power of the main beam and $dE_{sc}/dtdf$ is the power spectral density carried into the main beam by the scattered light. We can express $dE_{sc}/dtdf$ as

$$\frac{dE_{sc}}{dtdf} = \int_{\text{mirror}} P_{rec}\frac{dE_{sc}}{dtdAd\Omega df}(\lambda L)d\Omega ,$$

where $dE_{sc}/dtdAd\Omega df$ is the specific intensity of scattered light arriving at the receiving mirror, and λL is the area of the main beam on that mirror. Since we make no attempt to compute the relative phase $\Phi_{sc}-\Phi_{mb}$ of the scattered light and the main beam, we shall simply replace the cosine of that relative phase by its rms value, $1/\sqrt{2}$. By doing so and by using the standard relation

$$\tilde{h}(f) = \frac{1}{2\pi BL}\tilde{\Phi}_{mb}(f)$$

between the gravitational-wave noise and the main-beam phase noise (a relation which is essentially the definition of B), and by multiplying by a factor of $\sqrt{2}$ to account for the fact that scattered light can originate at either of the two ends of the vacuum pipe, we obtain the following formula for the gravitational-wave noise due to scattered light:

$$\tilde{h}(f) = \frac{\lambda}{2\pi BL}\left[\int P_{rec}(\theta)\frac{dE_{sc}/dtdAd\Omega df}{I/\lambda L}d\Omega\right]^{1/2} . \qquad (3.7)$$

Here and in the preceding equation the proportionality factor in front of the integral takes account of both arms: *The integral is to be performed at the corner mirror of only one arm, and the $\tilde{h}(f)$ which results is that for the entire detector.*

4. Reflection of Scattered Light off the Pipe Wall

In the remaining subsections of this section we shall discuss the interaction of scattered light with the wall of the vacuum pipe and with baffles, as it propagates from the scattering mirror to the receiving mirror. For each interaction process we shall describe the incoming light by the energy flux (power per unit area) $dE/dtdA$ of the unmodulated component of the incoming light, and by the specific energy flux (power per unit area per unit frequency) $dE/dtdAdf$ of the tiny portion that has been frequency-modulated by previous interactions with baffles and/or the wall. If the light has a well-defined propagation direction, then these energy fluxes carry all the relevant information. If there were a spread of propagation directions, then one would need to work with the intensity (flux per unit solid angle) $dE/dtdAd\Omega$ and specific intensity $dE/dtdAd\Omega df$.

Consider, first, the reflection of scattered light off the wall of the vacuum pipe. We shall treat such reflection as precisely specular (angle of reflection equals angle of incidence) and as lossless. (Losses are taken into account by placing the upper limit θ_o on angles of photons included in the analysis.)

Acoustical vibrations of the wall produce time variations (modulations) of the path length between the scattering and receiving mirrors, and corresponding modulations of the phase and thence frequency of the scattered light. In Sec. IV.A.4 [Eq. (4.19)] it is shown that the dominant contribution to the frequency modulation comes not from radial displacements ξ of the wall, but rather from changes in the longitudinal slope μ of the wall. The standard of reference for that slope is the line-of-site direction between two points: the point at which the reflecting light initiates its sequence of specular reflections, and the point at which it terminates them. Both of these points are baffles at which diffraction occurs, if both ends of the pipe are baffled; otherwise one or both points are the centers of interferometer mirrors. Correspondingly, if there are no baffles or only one end of the pipe is baffled, the modulations result from beam wiggle as well as from wall vibrations; but if both ends are baffled, wall vibrations are the sole source of the modulations.

The analysis of Sec. IV.A.4 shows that the frequency modulation put onto the light by the fluctuations in μ is described by

$$\Delta\frac{dE}{dtdAdf} = \frac{dE}{dtdA}\left[4\pi\tilde{\mu}\left[\frac{(L-2l)\theta + L\sqrt{L\theta/2R}\,\sigma_\mu}{\lambda}\right]\right]^2 . \tag{3.8}$$

Here $\tilde{\mu}^2(f)$ is the spectral density of μ, $dE/dtdA$ is the energy flux of the unmodulated component of scattered light, $\Delta(dE/dtdAdf)$ is the amount by which the tiny modulated component is augmented during the reflection, θ is the angle of the scattered light relative to the wall, $\bar{\mu}$ is the time-averaged slope of the wall, l is the distance of the reflection point from the scattering mirror, and in this version of the formula it is presumed that the scattering and receiving mirrors or diffracting baffles are at opposite ends of the pipe. For further discussion see Sec. IV.A.4.

5. *Diffraction of Scattered Light Off a Baffle*

Although the diffraction of light is a phenomenon that depends crucially on the phase differences of different propagation paths, in analyzing scattering we can embody the influence of those phase differences in a differential cross section $d\sigma/dxd\theta'$ and then use that cross section in a phase-ignorant intensity analysis. In this approach one must look carefully at phase when deriving formulas for $d\sigma/dxd\theta'$; but once that cross section has been derived, one can ignore phase when applying it.

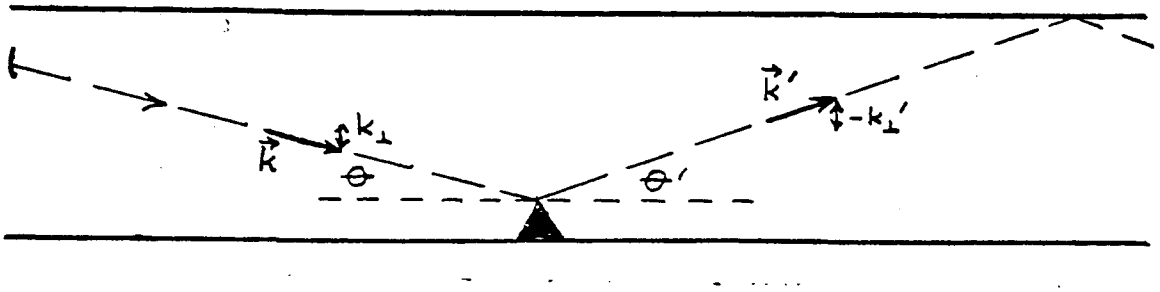

Fig. 3.1 Diffraction of light off a baffle. The long-dashed line is the path of a light ray. The projection of that path into the pipe wall cannot change in the diffraction: the angle θ relative to the wall changes into θ'.

The differential cross section $d\sigma/dxd\theta'$ is defined by the following formula in which one uses it: Suppose that light with wave vector $\vec{k}$ impinges on a baffle (Fig. 3.1). Then the diffracted light appears to emerge from the edge of the baffle. As for reflection off the wall, so also here, the component of the wave vector $\vec{k}_\parallel$ parallel to the wall is unchanged in the diffraction, while the component $k_\perp$ perpendicular can change. Define the angle of incidence by $\theta = k_\perp/k$ and the angle of diffraction by $\theta' = -k'_\perp/k$, where $\vec{k}'$ is the wave vector of the diffracted light. For wall reflection θ' must be equal to θ. For diffraction off a baffle θ' can have a range

of values. If the incoming light has energy flux $(dE/dtdA)_{in}$, then the power diffracted into a range $\Delta\theta'$ of θ' by a portion of baffle with length Δx is

$$\left[\frac{dE}{dt}\right]_{diff} = \left[\frac{dE}{dtdA}\right]_{in} \frac{d\sigma}{dx d\theta'} \Delta x \Delta\theta' . \tag{3.9}$$

The diffraction cross section $d\sigma/dx d\theta'$ is derived in Sec. IV.A.5. It depends only on the incoming angle θ, the outgoing angle θ', and the wavelength of the light:

$$\frac{d\sigma}{dx d\theta'} = \frac{\lambda}{4\pi^2} \frac{1}{(\theta+\theta')^2} . \tag{3.10}$$

Of particular interest will be light diffracted to angles θ' that are larger than the incoming angle θ. Most such light goes into angles $\theta' = (\text{several})\times\theta$; and the total cross section for diffraction into those angles is

$$\frac{d\sigma}{dx} = \int_0^{\pi/2} \frac{d\sigma}{dx d\theta'} d\theta' = \frac{\lambda}{8\pi^2} \frac{1}{\theta} . \tag{3.11}$$

The reason the differential cross section is given per unit linear angle θ' rather than per unit solid angle Ω' is that the components of $\vec{k}$ parallel to the wall are conserved; the diffraction is into a continuous range of θ' but not a continuous range of solid angle.

When light diffracts off a baffle, vibrations of the baffle frequency-modulate it. If $\xi^2(f)$ is the spectral density of the vertical displacement of the baffle, then the diffraction-produced augmentation of the specific flux of modulated light is

$$\Delta\left[\frac{dE}{dtdAdf}\right]_{diff} = \left[\frac{dE}{dtdA}\right]_{diff} [2\pi(\theta+\theta')\xi/\lambda]^2 ; \tag{3.12}$$

see Sec. IV.A.4 for a derivation.

6. Diffraction-Aided Reflection

The baffle configuration suggested in this report is designed to force all light with $\theta < \theta_o$ to encounter baffles. In addition to diffraction (treated above), there is one other important way by which light can escape being trapped by the baffles it encounters: the "diffraction-aided reflection" depicted in Fig. 3.2.

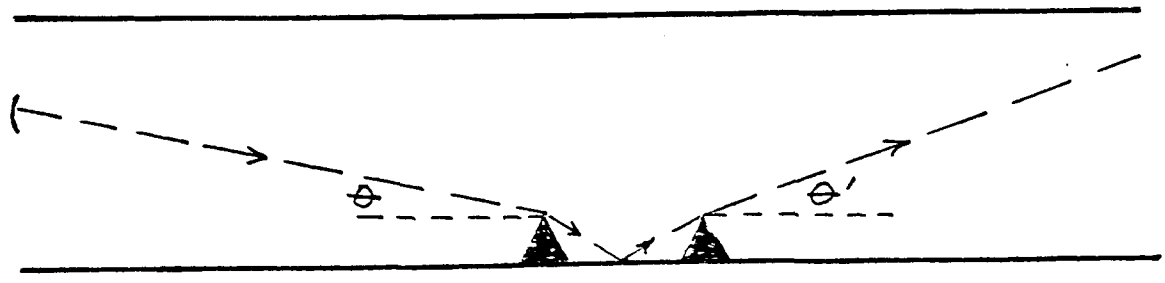

Fig. 3.2 Diffraction-aided reflection.

In this diffraction-aided reflection, light diffracts off the first of two baffles, bending its propagation downward sufficiently to be able to reflect specularly off the wall and then climb up above the top of the second baffle where it diffracts off into a more shallow angle. Here, as in ordinary diffraction, the trajectory of a light ray parallel to the wall cannot change. The only thing that changes is the angle θ between the wall and the ray; it goes from θ to some new angle θ'. Correspondingly, diffraction-aided reflection can be

described by the same type of cross section, $d\sigma/dx d\theta'$, as is used for ordinary diffraction.

A special role in the cross section will be played by the minimum angle

$$\theta_n \equiv \frac{H_n + H_{n+1}}{s_n} \tag{3.13}$$

that an incoming ray must have in order to successfully clear baffle n, then reflect specularly off the pipe wall, and then clear baffle $n+1$ without the aid of diffraction. Recommendation 1 of this report (Sec. II.1) guarantees that all light experience at least two baffle encounters in which

$$\theta_n - \theta \geq 2\delta H/s_n = \frac{2\delta H}{H_n + H_{n+1}}\theta_n \sim \frac{1}{5}\theta_n \ . \tag{3.14}$$

In such encounters pure reflection is severely impossible, but diffraction-aided reflection can occur and is larger than one naively might expect. We shall confine our discussion of the cross section $d\sigma/dx d\theta'$ to the regime (3.14) of baffle encounters.

I have computed the differential cross section $d\sigma/dx d\theta'$ for the regime (3.14). My result is given by the following set of formulas and is depicted in Fig. 3.3:

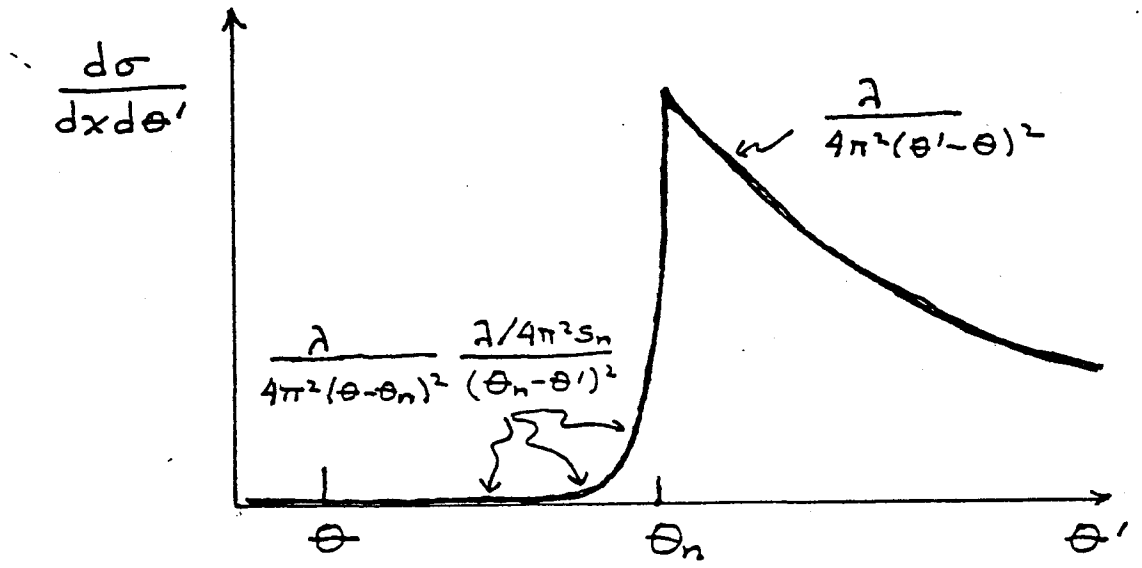

Fig. 3.3 The differential cross section for diffraction-aided reflection in the regime (3.14).

$$\frac{d\sigma}{dx d\theta'} = \frac{\lambda}{4\pi^2}\frac{1}{(\theta'-\theta)^2} \quad \text{for } \theta'-\theta_n \gg \left[\frac{\lambda}{4\pi^2 s_n}\right]^{1/2}$$

$$= \frac{\lambda}{4\pi^2(\theta-\theta_n)^2}\frac{\lambda/4\pi^2 s_n}{(\theta_n-\theta')^2} \quad \text{for } \theta'-\theta_n \ll -\left[\frac{\lambda}{4\pi^2 s_n}\right]^{1/2} . \tag{3.15}$$

This cross section is negligibly small for $\theta'-\theta_n \ll -\sqrt{\lambda/4\pi^2 s_n}$; and it rises sharply, at $|\theta'-\theta_n| \lesssim \sqrt{\lambda/4\pi^2 s_n}$, to its peak value. This and the fact that $\sqrt{\lambda/4\pi^2 s_n} \ll \theta_n - \theta$, permit us to approximate the cross section by

$$\frac{d\sigma}{dx d\theta} = 0 \quad \text{for } \theta < \theta' < \theta_n \ ,$$

$$= \frac{\lambda}{4\pi^2} \frac{1}{(\theta'-\theta)^2} \quad \text{for } \theta' > \theta_n \ ; \tag{3.16}$$

cf. Fig. 3.3. This cross section sends most of the diffracted photons into angles θ' between θ_n and θ_n+(several)×($\theta_n-\theta$); and the total cross section for sending light into that region is

$$\frac{d\sigma}{dx} = \int_0^{\pi/2} \frac{d\sigma}{dx\,d\theta'} d\theta' = \frac{1}{4\pi^2} \frac{\lambda}{\theta_n-\theta} \le \frac{1}{4\pi^2} \frac{\lambda s_n}{\delta H} \ . \tag{3.17}$$

Note that with our choice of baffle safety factor $\delta H = 1$ cm and baffle height $H = 5$ cm, this total cross section has $\theta_n = \theta/5$, and correspondingly it is a factor 2×5 = 10 times larger than the cross section (3.11) for ordinary diffraction. Note further than in the region of interest, $\theta' > \theta_n$, the value (3.16) of the differential cross section has a simple explanation: The light makes a single diffraction at the first baffle, to an angle $-\theta'$, then reflects off the wall (converting its angle from $-\theta'$ to $+\theta'$), then flies unhindered over the second baffle. Correspondingly, the cross section for this diffraction-aided reflection is precisely that (3.10) for ordinary diffraction, with θ' replaced by $-\theta'$.

We note in passing that, when one places no restrictions at all on the range of θ and θ' [i.e. when one abandons restriction (3.14)], the cross section $d\sigma/dx\,d\theta'$ *turns out to be symmetric* under interchange of the pair (θ,l_n) with the pair $(\theta',L-l_{n+1})$; see Sec. IV.A.6 for a proof. This means, as a special application, that the cross sections (3.15) and (3.16) are unchanged when θ and θ' are interchanged; i.e. they are unchanged when the direction of propagation of the ray in Fig. 3.2 is reversed.

Vibration of the wall and of the baffles in diffraction-aided reflection will modulate the frequency of the scattered light. The dominant modulation comes not from the vertical displacement ξ of the walls and baffles, but rather from the changes $\delta\theta = \delta\mu$, $\delta\theta' = -\delta\mu$ of the incoming and outgoing angles relative to the pipe wall. If $\tilde{\mu}^2(f)$ is the spectral density of $\delta\mu(t)$, then the modulation turns out to be [Eq. (4.38) of Sec. IV.A.6]

$$\Delta \frac{dE}{dt\,dA\,df} = \frac{dE}{dt\,dA} \left(\pi \frac{2L-l_n}{\lambda} \theta_o \tilde{\mu} \right)^2 . \tag{3.18}$$

7. Scattering by Baffles

A final process by which scattered light can interact with a baffle is by scattering off it. In such scattering the only regime of interest is that in which the incoming and outgoing rays are nearly parallel to the pipe's central axis (to within angles $\theta < \theta_o \lesssim 5$ degrees), and thus make angles of about 45 degrees to the baffle faces. We shall describe such scattering by the cross section $d\sigma$ per unit area of baffle dA to send incoming, near-45-degree photons back into a unit solid angle $d\Omega$ in a near-45-degree direction; and in numerical estimates we shall use for this cross section the conservative estimate

$$\frac{d\sigma}{dA\,d\Omega} \sim 0.1 \ . \tag{3.19}$$

In such baffle scattering the light will acquire the following frequency modulation due to longitudinal vibration of the baffles (cf. Sec. IV.A.4):

$$\Delta \frac{dE}{dA\,dt\,df} = \frac{dE}{dA\,dt} \left(4\pi \frac{\xi}{\lambda} \right)^2 . \tag{3.20}$$

B. LIGO With No Baffles

Suppose that baffles are not included in the vacuum pipe. How severe, then, will be the scattering noise? It is fairly obvious that without baffles the predominant way in which light can scatter out of the main beam, acquire a time varying phase shift, and then scatter back in again, is that shown in Fig. 3.4: The light leaves the main beam by scattering off a mirror; it then reflects specularly one or more times off the wall of the vacuum pipe, acquiring frequency modulation in each reflection; and it then propagates to the other mirror where it recombines with the main beam either via scattering or via transmission to the photodiode.

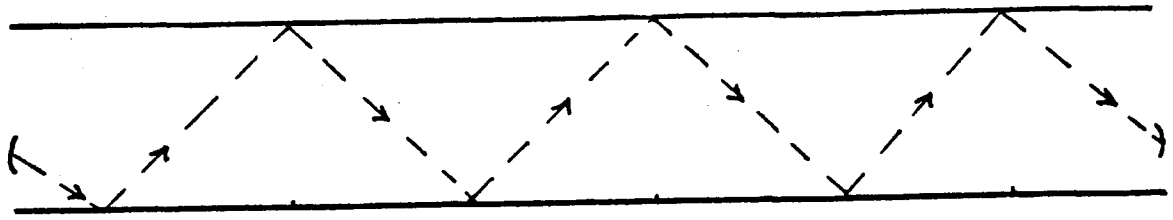

Fig. 3.4 The dominant scattering noise source for a LIGO without baffles: Light (dashed line) scatters off the end mirror, then reflects several times off the wall of the vacuum pipe, then propagates to the corner mirror. At the corner mirror it can propagate directly to the photodiode along with the main beam, or it can scatter back into the main beam and propagate as part of that beam toward the end mirror.

It is straightforward to use the intensity-analysis formulae developed in the last section to derive expressions for the noise due to this process. The derivation is sketched in Sec. IV.B, and the justification for ignoring phase coherence (i.e. for using intensity techniques) is discussed in Sec. IV.E and the paragraph following Eq. (4.11). The results are as follows:

1. Without Mode Cleaner

When there is no mode cleaner on the interferometer output, the recombination of the scattered light with the main beam is in the photodiode. The noise is dominated by scattered rays that have large angles $\theta - \theta_o$ and that thus bounce many times between the two mirrors. The analysis in Sec. IV.B gives for the noise

$$\tilde{h}(f) = \frac{\sqrt{2}}{\sqrt{3}} \frac{\sqrt{\alpha}(1-\bar{\eta})}{B} \left[\frac{\sqrt{\lambda L}}{R}\right]^{3/2} \theta_o \tilde{\mu}(f) . \tag{3.21}$$

For the set of numerical values listed at the beginning of Sec. III [$\alpha = 10^{-6}$, $\bar{\eta} = 0.9$, $B = 2000\,(10\,\mathrm{Hz}/f)$, $\lambda = 0.4\,\mu\mathrm{m}$, $L = 4\,\mathrm{km}$, $R = 60\,\mathrm{cm}$, $\theta_o = 0.1$ radians] Eq. (3.21) gives

$$\tilde{h}(f) = \frac{7\times10^{-20}}{\sqrt{\mathrm{Hz}}} \frac{\tilde{\mu}}{10^{-9}\,\mathrm{Hz}^{-1/2}(10\,\mathrm{Hz}/f)} . \tag{3.21'}$$

The form chosen for the spectral density of fluctuations in the angle μ,

$$\tilde{\mu} = 10^{-9}\,\mathrm{Hz}^{-1/2}(10\,\mathrm{Hz}/f) . \tag{3.22}$$

requires discussion. There are two independent sources of $\tilde{\mu}$: beam wiggle and acoustic noise on the vacuum pipe. *Acoustic noise:* The supports of the vacuum pipe are likely to vibrate at the level of the local seismic noise, $\tilde{\xi}_{\mathrm{seismic}} = 10^{-7}\,\mathrm{cm\,Hz}^{-1/2}\times(10\,\mathrm{Hz}/f)^2$. These vibrations will send acoustic waves down the pipe. If the free pipe responds somewhat resonantly to the motion of the supports, the pipe might have a displacement $\tilde{\xi}$ as much as 10 times larger than that of the supports, $\tilde{\xi}_{\mathrm{pipe}} = 10\tilde{\xi}_{\mathrm{seismic}}$. The sound speed for flexural motions of the pipe might be roughly 4×10^4 cm/sec, corresponding to a wavelength $\lambda_{\mathrm{sound}} = 4000\,\mathrm{cm}\,(10\,\mathrm{Hz}/f)$. These sound waves would then produce $\tilde{\mu} = 2\pi\tilde{\xi}_{\mathrm{pipe}}/\lambda_{\mathrm{sound}}$, which works out to be expression (3.22). *Beam wiggle:*

In a LIGO without baffles the points where the reflecting rays initiate and terminate their journeys are the mirror centers; and correspondingly μ is the slope of the wall relative to the main-beam axis. This means that beam wiggle shows up fully in $\tilde{\mu}$. It may be difficult, and perhaps impossible, to keep the beam wiggle as small as (3.22). If it is impossible, then the noise could be even larger than the estimate (3.21').

The estimate (3.21') of the scattering noise without mode cleaner is 2×10^4 times larger than the standard quantum limit at 10 Hz and 2×10^5 times larger at 100 Hz. This strongly motivates including baffles in the LIGO and designing them to reduce the scattering noise by a factor of at least 10^5.

2. With Mode Cleaner

With a mode cleaner on the interferometer, the recombination mechanism is scattering off the receiving mirror, and the noise works out to be (Sec. IV.B)

$$\tilde{h} = \frac{2}{\sqrt{3}}\frac{\alpha}{B}\left[\frac{\sqrt{\lambda L}}{R}\right]^{3/2}\left[\frac{\lambda}{L}\right]^{1/4}\theta_o^{1/2}\tilde{\mu}\ . \tag{3.23}$$

The presence of θ_o in this formula is a signal that, as without a mode cleaner, the noise is dominated by large-angle scatterings which entail many reflections on the vacuum pipe. Numerically, with the parameter values listed above, this works out to be

$$\tilde{h} = \frac{1\times10^{-23}}{\sqrt{\text{Hz}}}\frac{\tilde{\mu}}{10^{-9}\,\text{Hz}^{-1/2}(10\,\text{Hz}/f)}\ . \tag{3.23'}$$

For the chosen parameter values this is a factor 2 larger than the standard quantum limit at 10 Hz and a factor 20 larger at 100 Hz. Any temptation that this "smallness" of the noise might give to build the LIGO without baffles should be mitigated by the following: (i) We do not now know whether it will be possible to use a mode cleaner on the output in a sufficiently noise-free way to permit bringing the scattering noise down to this level. (ii) Even with a successful mode cleaner, expression (3.23) could actually underestimate the noise by a factor 10 or so.

Nevertheless, it is encouraging that a mode cleaner can be so effective in bringing scattering noise under control, and that the noise level might be as low as (3.23), even in the absence of baffles.

C. LIGO With Baffles: Diffraction-Aided Reflection

Throughout the rest of Sec. III we shall presume that baffles are incorporated in the LIGO in the configuration suggested in Sec. II.1, with constant baffle heights $H_n = H$. The first baffle is at a distance $l_1 \geq 10$ meters from the plane of the corner mirror; there is then a first series of $R/(H-\delta H)$ baffles with equal spacings

$$s_n = \frac{2(H-\delta H)}{\theta_o}\ ; \tag{3.24a}$$

and there is then a second series of $[R/(H-\delta H)]\ln(\theta_o L/4R)$ baffles extending up to the center of the vacuum pipe, with spacing

$$s_n = \frac{H-\delta H}{R}(l_n - l_1) \tag{3.24b}$$

between baffle n and baffle $n+1$.

We shall consider two possibilities: that there are no baffles in the outer half of the vacuum pipe; and that there is a full set configured in the same manner as (3.24), but beginning from the end mirror. We shall concern ourselves only with noise in full-length detectors. The half-length detectors benefit only from the

baffles of the inner half pipe and thus are a special case of the one-set-of-baffles formulae.

In the case of one set of baffles, the dominant scattering noise involves photons that do one of two things (Fig. 3.5a): (i) scatter off the corner mirror at some angle θ, then circumvent the first pair of baffles they encounter by means of diffraction-aided reflection to a slightly larger angle $\theta' \sim \theta + (\text{several}) \times (\theta_n - \theta) \sim 1.5\theta$, then reflect repeatedly off the pipe wall (acquiring frequency modulation at each reflection) until they reach the end mirror where they recombine with the main beam by scattering; or (ii) trace precisely the reverse route: scatter off the end mirror at an angle θ', reflect multiple times off the pipe wall, circumvent the first troublesome set of baffles by a diffraction-aided reflection to angle θ, then fly directly to the corner mirror and there recombining with the main beam either by scattering or by transmission to the photodiode.

In the case of two sets of baffles, the dominant scattering noise involves photons which follow routes identical to the one-set-of-baffles case with one exception: The reflection nearest each of the two ends of the pipe must be diffraction-aided (Fig. 3.5b). [*Note*: There is also noise due to these same processes but with diffraction-aided reflection replaced by ordinary diffraction. However, because the cross section for ordinary diffraction is ~1/10 that for diffraction-aided reflection, it can be neglected. Diffraction-aided reflection dominates the noise.]

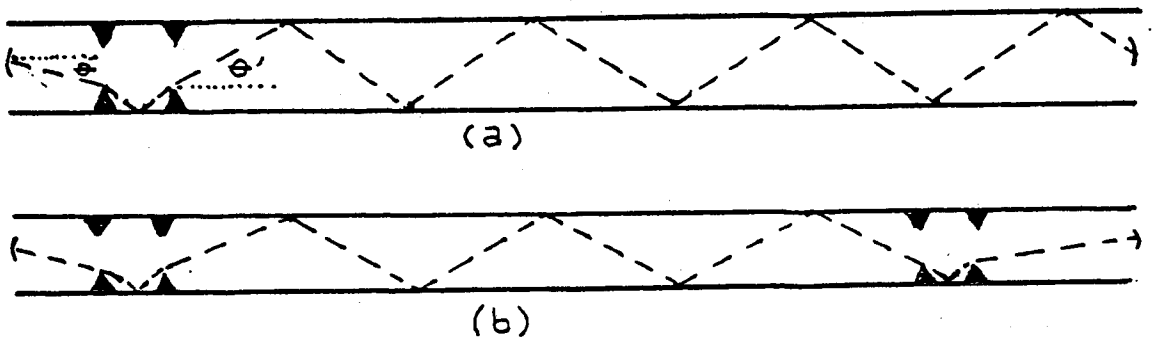

Fig. 3.5 The dominant scattering noise sources for a LIGO with baffles: (a) For a pipe with just one set of baffles. The photons responsible for the noise trace out the dashed route in either direction. In this route the wall-reflection nearest the corner mirror is diffraction aided; all other reflections are ordinary and specular. (b) For a pipe with two set of baffles, one in each end of the pipe. In this case the noise-producing photons undergo two diffraction-aided reflections: one at each end of the pipe.

The noise due to the processes in Fig. 3.5 is computed in Sec. IV.C using the amplitude-analysis formulae of Sec. III.A. We shall discuss the results of the computation in the following two subsections — first for detectors without mode cleaners, then for detectors with mode cleaners.

1. Without Mode Cleaner

For a LIGO with baffles the noise is the worst when the mirrors are near the edge of the vacuum pipe, because it then is easier to circumvent the first pair of baffles encountered (the required diffraction angle, $\theta_n - \theta$, is smaller and thus the cross section for diffraction-aided reflection is higher). For such near-the-wall mirrors the noise is

$$\tilde{h} = \left[\frac{1}{24\pi^2}\frac{\lambda}{\delta H}\right]^{1/2} \frac{\sqrt{\alpha}(1-\bar{\eta})}{B}\left[\frac{\sqrt{\lambda L}}{R}\right]^{3/2} \theta_o^{1/2}\,\tilde{\mu}$$

$$= \frac{1\times10^{-22}}{\sqrt{\text{Hz}}}\,\frac{\tilde{\mu}}{10^{-9}\,\text{Hz}^{-1/2}(10\,\text{Hz}/f)} \quad \text{for one set of baffles,} \tag{3.25a}$$

$$\tilde{h} = \frac{1}{\sqrt{3}} \frac{1}{16\pi^2} \frac{\lambda}{\delta H} \frac{\sqrt{\alpha(1-\bar{\eta})}}{B} \left[\frac{\sqrt{\lambda L}}{R}\right]^{3/2} \left[\ln\left(\frac{L\theta_o}{4R}\right)\right]^{1/2} \tilde{\mu}$$

$$= \frac{3\times 10^{-25}}{\sqrt{\text{Hz}}} \frac{\tilde{\mu}}{10^{-9}\,\text{Hz}^{-1/2}(10\,\text{Hz}/f)} \quad \text{for two sets of baffles.} \tag{3.25b}$$

The dependences on the maximum possible photon angle θ_o and the minimum possible angle $4R/L$ indicate that with one set of baffles the dominant noise is due to large-angle, many-reflection photons, while with two sets of baffles photons of large angles and small contribute equally. Note that the improvement in noise over the no-baffle LIGO is a factor 10^3 with one set of baffles and 3×10^5 with two sets. With one set the computed noise is a factor 25 larger than the standard quantum limit at 10 Hz and 250 larger at 100 Hz, for the chosen parameter values; with two sets it is 10 times smaller than the standard quantum limit at 10 Hz and at the standard quantum limit at 100 Hz. These numbers are one motivation for the recommendation to use two sets of baffles.

A second motivation for two sets of baffles is to reduce the sensitivity of the noise to beam wiggle: The $\tilde{\mu}$ that appears in the noise formulae (3.25) is (the square root of the spectral density of) the angle of the pipe at reflection points. In Eqs. (3.25) this pipe angle is measured relative to the line of sight between the points where the reflecting photons initiate and terminate their specular-reflection motion. Those initial and terminal points in the case of a LIGO with no baffles (Sec. III.B) are the two mirrors; $\tilde{\mu}$ therefore is the angle between the main beam and the pipe wall; and $\tilde{\mu}$ thus is fully sensitive to beam wiggle. When there is one set of baffles, the initial and terminal points for photon reflections are one mirror and the one baffle pair at which the diffraction-aided reflection occurs. Thus, lateral motion of the main beam on the mirror (beam wiggle) again shows up in $\tilde{\mu}$, but with a modestly reduced influence. When there are two sets of baffles, the initial and terminal points for the photon reflections are the two baffle pairs — one near each end of the pipe — at which the two diffraction-aided reflections occur. In this case, sensitivity of $\tilde{\mu}$ to beam wiggle is strongly reduced. I have not attempted to compute the actual reduction factor, but I would expect it to be several orders of magnitude. Since controlling beam wiggle at the level 10^{-9} radians/$\text{Hz}^{1/2}\times(10\,\text{Hz}/f)$ is likely to be very difficult and perhaps impossible, this reduction of sensitivity to beam wiggle seems to me very important.

Expression (3.8) reveals that the modulation of scattered light by reflection (proportional to $\sqrt{dE/dtdAdf}$) is second order in small angles. (It nevertheless is the dominant form of modulation because the pipe length L acts like a "lever arm" to amplify the modulation.) There are two second-order contributions to the modulation: one proportional to $\theta\,\tilde{\mu}$ (product of scattered-photon angle with fluctuations of wall angle), and one proportional to $\sigma_{\mu_*}\tilde{\mu}$ (product of rms wall angle with fluctuations of wall angle). The noise levels quoted above are those of the "$\theta\,\tilde{\mu}$" noise. For comparison, the "$\sigma_{\mu_*}\tilde{\mu}$" noise is given by

$$\frac{\tilde{h}_{\mu_*}}{\text{expression (3.25a)}} = \frac{3\sigma_{\mu_*}}{\sqrt{\theta_o(4R/L)}}\left[\ln\left(\frac{L\theta_o}{4R}\right)\right]^{1/2} = \frac{\sigma_{\mu_*}}{0.001} \quad \text{for one set of baffles,} \tag{3.26a}$$

$$\frac{\tilde{h}_{\mu_*}}{\text{expression (3.25b)}} = \frac{3\sigma_{\mu_*}}{(4R/L)\sqrt{\ln(L\theta_o/4R)}} = \frac{\sigma_{\mu_*}}{5\times 10^{-4}} \quad \text{for two sets of baffles.} \tag{3.26b}$$

This and the corresponding formula (3.28) below for a detector with mode cleaner motivate the recommended upper limit on fluctuations in straightness and circularity of the pipe walls [Eq. (2.7)].

2. With Mode Cleaner

When a mode cleaner is used on the detector's output, the noise works out to be (see Sec. IV.C)

$$\tilde{h} = \left[\frac{1}{24\pi^2}\frac{\lambda}{\delta H}\right]^{1/2}\frac{\alpha}{B}\left[\frac{\sqrt{\lambda L}}{R}\right]^{3/2}\left[\frac{\lambda}{L}\right]^{1/4}\left[\ln\left[\frac{L\theta_o}{4R}\right]\right]^{1/2}\tilde{\mu}$$

$$= \frac{2\times10^{-26}}{\sqrt{\text{Hz}}}\,\frac{\tilde{\mu}}{10^{-9}\,\text{Hz}^{-1/2}(10\,\text{Hz}/f)} \quad \text{for one set of baffles,} \tag{3.27a}$$

$$\tilde{h} = \frac{1}{\sqrt{3}}\frac{1}{64\pi^2}\frac{\lambda}{\delta H}\frac{\alpha}{B}\left[\frac{\sqrt{\lambda L}}{R}\right]^2\tilde{\mu}$$

$$= \frac{1\times10^{-28}}{\sqrt{\text{Hz}}}\,\frac{\tilde{\mu}}{10^{-9}\,\text{Hz}^{-1/2}(10\,\text{Hz}/f)} \quad \text{for two sets of baffles.} \tag{3.27b}$$

The dependences on angles indicate that for one set of baffles all photon angles θ, from θ_o down to $\sim 4R/L$, are significant contributors; while for two sets of baffles the smallest angles, $\theta \sim 4R/L$ (those with only a few reflections), dominate.

For the chosen parameters the noise reductions due to including baffles are ~ 500 with one set of baffles, and ~ 10^5 with two sets. The computed noise levels are several orders of magnitude below the standard quantum limit — sufficiently far below that we should feel quite comfortable. If we were sure that mode cleaners could be implemented on the interferometer output at the exquisitely good sensitivities we are discussing, we might even live happily with just one set of baffles — until we reminded ourselves of the issue of sensitivity to beam wiggle. Then we might hesitate.

With a mode cleaner present, noise associated with fluctuations in the pipe's straightness and roundness ("$\mu_o\tilde{\mu}$" noise) has the magnitude

$$\frac{\tilde{h}_{\mu_o}}{\text{expression (3.27a)}} = \frac{3\sigma_{\mu_o}}{(4R/L)\sqrt{\ln(L\theta_o/4R)}} = \frac{\sigma_{\mu_o}}{5\times10^{-4}} \quad \text{for one set of baffles ,} \tag{3.28a}$$

$$\frac{\tilde{h}_{\mu_o}}{\text{expression (3.27b)}} = \frac{3\sigma_{\mu_o}}{\sqrt{2}\,(4R/L)} = \frac{\sigma_{\mu_o}}{3\times10^{-4}} \quad \text{for two sets of baffles .} \tag{3.28b}$$

Thus, if the rms fluctuations in straightness and roundness are much larger than 10^{-3}, the "$\mu_o\,\tilde{\mu}$" noise [Eqs. (3.28) and (3.26)] will be significantly larger than the "$\theta\,\tilde{\mu}$" noise [Eqs. (3.27) and (3.25)]. This is the origin of the recommended upper limit (2.7) on straightness and roundness of the vacuum pipe.

This entire discussion is based on the assumption that coherent superposition of light is unimportant in the dominant scattering processes of Fig. 3.5. We shall examine this assumption in Sec. IV.E and shall discuss there the need for jaggedness of the baffle edges to protect against coherence.

D. LIGO With Baffles: Scattering of Light off the Baffles

When baffles are present the most dangerous source of noise, aside from diffraction-aided reflection, is the baffles' rescattering of light directly back to the mirror from which it came (Fig. 3.6). This rescattered light gets frequency-modulated by longitudinal vibrations $\tilde{\xi}(f)$ of the baffles. The resulting noise, as computed in Sec. IV.D, is discussed in the next two subsections:

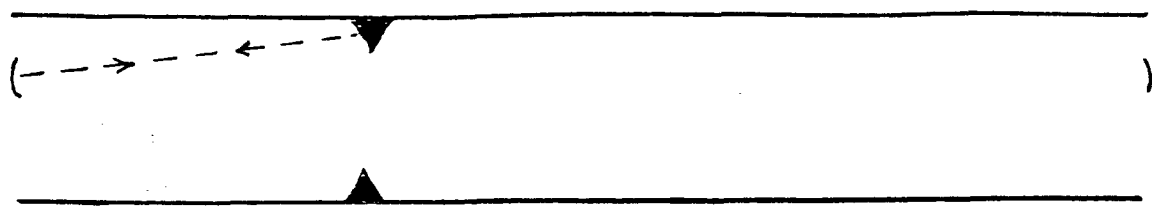

Fig. 3.6 Main-beam light scatters off a mirror toward a baffle, then scatters off the face of the baffle directly back to the mirror where it recombines with the main beam.

1. Without Mode Cleaner

When there is no mode cleaner on the output, the dominant noise is due to the baffles which are nearest the scattering mirror — and thus it is sensitive to the distance l_1 from the mirror to the first baffle. The noise is also stronger, the smaller is the photon angle θ to reach the nearest part of that baffle; and thus it is sensitive to the transverse distance Y_o between the mirrors' main beam and the edge of the baffle. For two sets of baffles the noise works out to be

$$\tilde{h} = \frac{2\sqrt{\alpha}(1-\bar{\eta})}{B}\left[\frac{d\sigma}{dA\,d\Omega}\right]^{1/2}\left[\frac{\lambda}{L}\right]^{1/4}\left[\frac{\sqrt{\lambda L}}{Y_o}\right]\left[\frac{\sqrt{\lambda L}}{l_1}\right]^{1/2}\left[\frac{R}{\sqrt{\lambda L}}\right]^{1/2}\frac{\xi}{L}$$

$$= \frac{1\times10^{-24}}{\sqrt{\text{Hz}}}\left[\frac{10\,\text{Hz}}{f}\right]\left[\frac{\xi}{10^{-7}\,\text{cm}\,\text{Hz}^{-1/2}(10\,\text{Hz}/f)^2}\right]; \qquad (3.29)$$

for one set of baffles the noise is smaller by $1/\sqrt{2}$. The number shown assumes $Y_o = 5\sqrt{\lambda L} = 20\,\text{cm}$, and also $l_1 = 10\,\text{meters}$, the smallest mirror-baffle distance allowed by Recommendation 1 of Sec. I. In fact, the noise level (3.29) is the motivation for the limit $l_1 > 10\,\text{meters}$ in Recommendation 1. With $l_1 = 10\,\text{meters}$ the noise, (3.29), is 1/4 of the standard quantum limit. This is about as close to the limit as it seems wise to go. Smaller l_1 would put us closer.

2. With Mode Cleaner

When a mode cleaner is used on the output, all baffles contribute roughly equally to the rescattering noise, and the noise works out to be

$$\tilde{h} = \frac{2\sqrt{2}\alpha}{B}\left[\frac{d\sigma}{dA\,d\Omega}\right]^{1/2}\left[\frac{\lambda}{L}\right]^{1/2}\left[\frac{\sqrt{\lambda L}}{Y_o}\right]^{3/2}\left[\frac{H}{\sqrt{\lambda L}}\right]^{1/2}N_b^{1/2}\frac{\xi}{L}$$

$$= \frac{1\times10^{-27}}{\sqrt{\text{Hz}}}\left[\frac{10\,\text{Hz}}{f}\right]\left[\frac{\xi}{10^{-7}\,\text{cm}\,\text{Hz}^{-1/2}(10\,\text{Hz}/f)^2}\right]. \qquad (3.30)$$

This is a factor 4000 below the standard quantum limit — very comfortable.

E. LIGO With Baffles: Mirrors Near the Pipe's Center

If the pipe were perfectly straight and round and the baffles were not jagged, then for mirrors at the pipe's center the noise would be strongly enhanced due to two effects: (i) The pipe would act like a mirror to focus scattered light from one interferometer mirror onto the center of the other, thereby increasing the intensity of the light and increasing its noise. (ii) Because the diffracting baffles would be symmetric with respect to the mirrors, the Fresnel patterns would be unable to suppress coherent effects; and coherence would further enhance the noise. Crookedness of the pipe, deformations of the pipe from roundness, and jaggedness of the

baffles are the methods of controlling these noise enhancements.

Crookedness is characterized by transverse displacements $\vec{\xi}_o$ of the central axis of the pipe from a perfectly straight line. The rms value of this displacement we denote by σ_{ξ_o}; and we assume for numerical purposes that $\sigma_{\xi_o} = 1$ cm. In this section I shall quantify the suppression of noise by this crookedness; see Sec. IV.E for derivations. I am quite sure that the suppression by deformations from roundness is of the same magnitude as suppression by crookedness; i.e. in the following equations one should replace σ_{ξ_o} by $\sqrt{\sigma_{\xi_o}^2+\sigma_{\xi_2}^2}$ where σ_{ξ_2} is the rms amplitude of the quadrupolar ($m = 2$) deformations of the pipe from roundness. However, I have not proved that this is so. In any event, even without any deviations from roundness, the crookedness alone should lead to the following levels of noise suppression.

The jaggedness of the baffles will be described by the maximum wavelength σ_H of the jags. The height of the jags is not important, so long as it is larger than the minimum given by Eq. (2.6).

A role similar to that of jaggedness is played by spatial phase fluctuations due to the nonzero coherence lengths of (i) the mirror irregularities which produce scattering and recombination, and (ii) the photodiode irregularities which produce recombination. The transverse wavelengths of these phase fluctuations evaluated at the midpoint of the pipe's length (i.e. at baffles that are roughly equidistant from the two ends) we shall denote σ_M and σ_{pd}. These wavelengths are expressed in terms of the coherence lengths of the mirror and photodiode irregularities by Eqs. (4.5d) and (4.11) with $z = z' = L/2$; and they have magnitudes $\sigma_M \gtrsim \sqrt{\lambda L}$, $\sigma_{pd} \gtrsim \sqrt{\lambda L}$.

In discussing the noise we shall examine first noise due to light that does not reflect off the walls at all; i.e. light that scatters from one mirror, diffracts off one baffle, then recombines with the main beam at the other mirror; see Fig. 4.7 below. We shall call this "diffraction without reflection". Then we shall examine the noise due to light that both diffracts and reflects (Fig. 3.5 for mirrors at the pipe's center).

1. Diffraction Without Reflection

It is shown in Sec. IV.E.1 using a phase-coherent (amplitude) analysis that, for mirrors that are precisely at the pipe's center and for precisely centered baffles (no pipe offset $\vec{\xi}_o$ at the baffle locations), the noise due to diffraction without reflection is given by

$$\tilde{h} = \frac{\sqrt{\bar{\alpha}(1-\bar{\eta})}}{B}\left[\frac{\lambda}{L}\right]^{1/2}\left[\frac{\sqrt{\lambda L}}{R}\right]^{1/2}\left[\frac{R}{H-\delta H}\right]^{1/2}\left[\frac{L\theta_o}{R}\right]^{1/2}\left[\frac{\min(\sigma_M,\sigma_{pd},\sigma_H)}{2\pi R}\right]^{1/2}\frac{\xi}{L}$$

$$= \frac{3\times10^{-24}}{\sqrt{\text{Hz}}}\left[\frac{10\text{ Hz}}{f}\right]\left[\frac{\min(\sigma_M,\sigma_{pd},\sigma_H)}{2\pi R}\right]^{1/2}\frac{\xi}{10^{-7}\text{ cm Hz}^{-1/2}(10\text{ Hz}/f)^2}\,. \qquad (3.31a)$$

This is the noise in the absence of a mode cleaner. When a mode cleaner is present the noise is

$$\tilde{h} = \frac{\alpha}{B}\left[\frac{\lambda}{L}\right]^{1/2}\left[\frac{\sqrt{\lambda L}}{R}\right]\sqrt{N_b}\left[\frac{\min(\sigma_M,\sigma_H)}{2\pi R}\right]^{1/2}\frac{\xi}{L}$$

$$= \frac{1\times10^{-27}}{\sqrt{\text{Hz}}}\left[\frac{10\text{ Hz}}{f}\right]\left[\frac{\min(\sigma_M,\sigma_{pd},\sigma_H)}{2\pi R}\right]^{1/2}\frac{\xi}{10^{-7}\text{ cm Hz}^{-1/2}(10\text{ Hz}/f)^2}\,. \qquad (3.31b)$$

where N_b, the number of baffles, is given by Eq. (2.5). In these equations ξ is the square root of the spectral density of the radial baffle vibrations. With a mode cleaner present [Eq. (3.31b)] the noise is negligible whether or not the baffles are jagged. Without a mode cleaner [Eq. (3.31a)], the noise is about at the level of the quantum limit in the case of perfectly smooth baffles and large σ_M and σ_{pd}. One reason for baffle jaggedness is to drive this noise well below the quantum limit: With the recommended $\sigma_H \lesssim 5$ mm (Sec. II), the

baffle suppression factor will be $\sqrt{\sigma_H/2\pi R} \lesssim 0.04$. Pipe offset $\vec{\xi}_o$ at the baffles (i.e. pipe crookedness) will also suppress the noise a bit; but I have not calculated the amount of suppression.

2. Diffraction With Reflection

It is shown in Sec. IV.E.2 using a phase-coherent (amplitude) analysis that, for mirrors that are precisely at the pipe's center, the noise due to reflection combined with diffraction [both ordinary diffraction (Fig. 3.1) and diffraction-aided reflection (Fig. 3.5)] is given by the following expressions:

i. For one set of baffles and no mode cleaner

$$\tilde{h} = \frac{1}{7}\frac{\sqrt{\alpha}(1-\bar{\eta})}{B}\left[\frac{\lambda}{L}\right]^{1/2}\left[\frac{\sqrt{\lambda L}}{R}\right]^{1/2}\left[\frac{\sqrt{\lambda L}}{H}\right]^{1/2}\left[\frac{\sqrt{\lambda L}}{\sigma_\xi}\right]^{1/2}\left[\left[\frac{L\theta_o}{2R}\right]^{1/4} S\left[\frac{4(L\theta_o/2R)^{3/2}\sigma_\xi \sigma_H}{\lambda L}\right] + \frac{\sigma_\mu}{R} S\left[\frac{8\sigma_H\sigma_\xi}{\lambda L}\right]\right]\tilde{\mu}$$

$$= \frac{1\times10^{-22}}{\sqrt{\text{Hz}}}\,\frac{\tilde{\mu}}{10^{-9}\,\text{Hz}^{-1/2}(10\,\text{Hz}/f)}\left[S\left[\frac{\sigma_H}{6\times10^{-4}\,\text{cm}}\right] + \frac{\sigma_\mu}{6\times10^{-4}} S\left[\frac{\sigma_H}{2\,\text{cm}}\right]\right] . \tag{3.32a}$$

ii. For two sets of baffles and no mode cleaner

$$\tilde{h} = \frac{1}{180}\frac{\sqrt{\alpha}(1-\bar{\eta})}{B}\left[\frac{\lambda}{L}\right]^{1/2}\left[\frac{\sqrt{\lambda L}}{R}\right]\left[\frac{\sqrt{\lambda L}}{H}\right]\left[\frac{\sqrt{\lambda L}}{\sigma_\xi}\right]^{1/2}\left[1+\frac{2}{3}\frac{\sigma_\mu}{R/L}\right] S\left[\frac{8\sigma_\xi\sigma_H}{\lambda L}\right]\tilde{\mu}$$

$$= \frac{3\times10^{-25}}{\sqrt{\text{Hz}}}\,\frac{\tilde{\mu}}{10^{-9}\,\text{Hz}^{-1/2}(10\,\text{Hz}/f)}\left[1+\frac{\sigma_\mu}{2\times10^{-4}}\right] S\left[\frac{\sigma_H}{2\,\text{cm}}\right] . \tag{3.32b}$$

iii. For one set of baffles and a mode cleaner

$$\tilde{h} = \frac{1}{7}\frac{\alpha}{B}\left[\frac{\lambda}{L}\right]^{1/2}\frac{\sqrt{\lambda L}}{R}\left[\frac{\sqrt{\lambda L}}{H}\right]^{1/2}\left[\frac{\sqrt{\lambda L}}{\sigma_\xi}\right]^{1/2}\left[1+\frac{\sigma_\mu}{\sqrt{2}R/L}\right] S\left[\frac{8\sigma_\xi\sigma_H}{\lambda L}\right]\tilde{\mu}$$

$$= \frac{8\times10^{-26}}{\sqrt{\text{Hz}}}\,\frac{\tilde{\mu}}{10^{-9}\,\text{Hz}^{-1/2}(10\,\text{Hz}/f)}\left[1+\frac{\sigma_\mu}{2\times10^{-4}}\right] S\left[\frac{\sigma_H}{2\,\text{cm}}\right] . \tag{3.33a}$$

iv. For two sets of baffles and a mode cleaner

$$\tilde{h} = \frac{1}{25}\frac{\alpha}{B}\left[\frac{\lambda}{R}\right]^{1/2}\left[\frac{\sqrt{\lambda L}}{R}\right]^{3/2}\left[\frac{\sqrt{\lambda L}}{H}\right]\left[\frac{\sqrt{\lambda L}}{\sigma_\xi}\right]^{1/2}\left[1+\frac{\sigma_\mu}{R/L}\right] S\left[\frac{8\sigma_\xi\sigma_H}{\lambda L}\right]\tilde{\mu}$$

$$= \frac{5\times10^{-27}}{\sqrt{\text{Hz}}}\,\frac{\tilde{\mu}}{10^{-9}\,\text{Hz}^{-1/2}(10\,\text{Hz}/f)}\left[1+\frac{\sigma_\mu}{1.5\times10^{-4}}\right] S\left[\frac{\sigma_H}{2\,\text{cm}}\right] . \tag{3.33b}$$

In these formulas $S(x)$ is a function which describes the effects of jaggedness of the baffles. I have not computed the precise form of $S(x)$; however, considerations developed in Sec. IV.E.2 show that (i) it is always unity (there is no suppression of noise by jaggedness) when the argument x of $S(x)$ is greater than one:

$$S(x) = 1 \quad \text{for } x > 1 ; \tag{3.34a}$$

(ii) it is less than unity (there is noise suppression by jaggedness) when x is less than one

$$S(x) < 1 \quad \text{for } x < 1 ; \tag{3.34b}$$

(iii) the precise amount of suppression depends on the spectrum of the jaggedness (the distribution of wavelengths present); (iv) if the spectrum of the jaggedness is very small for wavelengths greater than the wavelength σ_H, then

$$S(x) \ll 1 \quad \text{for } x \ll 1 . \tag{3.34c}$$

For further details see Eqs. (4.93) and associated discussion.

Discussion

Equation (3.33a) shows that, when a mode cleaner is used and the rms beam-pipe offset is $\sigma_\xi = 1$ cm, then a single set of baffles might be sufficient to suppress diffraction-plus-reflection noise. The word "might" is because with just one set of baffles $\tilde{\mu}$ is sensitive to beam wiggle, and it is far from clear that $\tilde{\mu}$ can then be held to the level $\tilde{\mu} \lesssim 10^{-9}\,\mathrm{Hz}^{-1/2}\,(10\,\mathrm{Hz}/f)$. If it cannot be held to this level, and there is only one set of baffles, then significant noise suppression will have to be achieved via baffle jaggedness.

Since it is not certain that a mode cleaner can be implemented on the output at the sensitivity levels we require, we should be sure that the LIGO design also suppresses the noise adequately in the absence of a mode cleaner. Equation (3.32a) shows that it does not do so if there is just one set of baffles. The noise level (3.32a) is a factor 25 larger than the standard quantum limit at 10 Hz, and 250 times larger at 100 Hz. Moreover, the "$\theta\tilde{\mu}$" portion of the noise (the part not proportional to σ_{μ_o}) is incapable of being reduced by baffle jaggedness — unless the angle θ_o can be reduced far below 0.1. The reason is that this part of the noise [by contrast with all others in Eqs. (3.32) and (3.33)] is dominated by baffles near the ends of the pipe; and for those baffles jaggedness has an influence only when its wavelength is smaller than the extremely small value of $6\times10^{-4}\,\mathrm{cm}(0.1/\theta_o)^{3/2}$. This "$\theta\tilde{\mu}$" part of the noise also is not very susceptible to reduction by "blackening" of the pipe, i.e. by reduction of the angle θ_o, because it is proportional only to $\theta_o^{1/4}$. Thus, the only secure way of reducing this noise below the quantum limit is by using two sets of baffles [Eq. (3.32b)]. The second set of baffles drives down the noise due to end baffles so much that the central baffles come to dominate; and for them baffle jaggedness could be a significant help in reducing the noise below the $3\times10^{-25}\,\mathrm{Hz}^{-1/2}$ level — which, itself, is already below the quantum limit.

To recapitulate, for mirrors near the center of the pipe it is particularly important to have two sets of baffles. With two sets, the combination of crookedness of the pipe ($\sigma_\xi = 1$ cm), and baffle jaggedness can push the noise well below the quantum limit. In fact, crookedness alone brings the scattering noise for centered mirrors down to the level of that for mirrors near the pipe's walls [compare Eqs. (3.32) with Eqs. (3.25) and (3.26); also compare Eqs. (3.33) with Eqs. (3.27) and (3.28)].

IV. Derivation of the Formulas for Scattering Noise

This section sketches the derivation of the scattering-noise formulas given in Sec. III. Section IV.A derives intensity-analysis formulas for the specific processes discussed in Sec. III.A. Then Secs. IV.B, C and D derive the scattering formulas given above in Sections III.B, C and D respectively. Finally Sec. IV.E analyzes and discusses the possible roles of coherence in scattering noise and the role of baffle jaggedness in controlling coherent effects.

A. Formulas for Use in Intensity Analyses of Scattering

1. Scattering of Main Beam Off Mirror

The experimental basis for the scattering formula $P_{sc}(\theta) = \alpha/\theta^2$ and the parameter value $\alpha = 10^{-6}$ were explained in Sec. III.A.1. In this section we shall examine the relationship of this scattering probability to irregularities in the mirror, and we shall develop an amplitude analysis of the scattering (by contrast with the intensity analysis of Sec. III.A.1). Figure 4.1 is a foundation for our discussion.

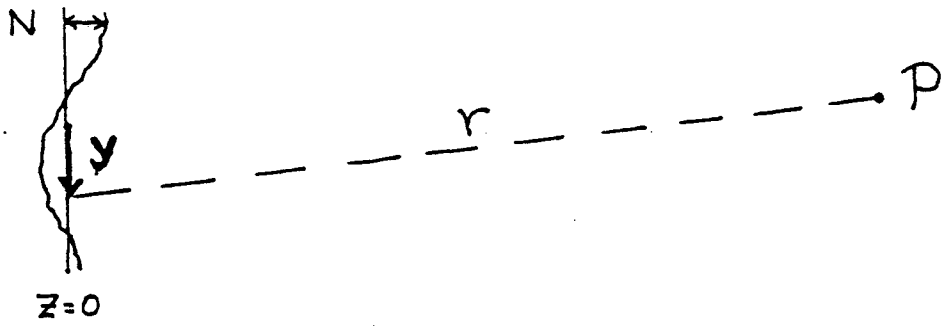

Fig. 4.1 The scattering of the main beam off irregularities in a flat mirror.

In Fig. 4.1 and our analysis we presume (for simplicity and without significant ultimate error) the following: (i) The mirror is flat rather than curved (aside from its irregularities discussed below). (ii) The light is describable by a scalar field (an appropriate component of its electric field, appropriately renormalized) that is sinusoidal in time with angular frequency ω and wave number $k = \omega/c = 2\pi/\lambda$ and with spatial form $\psi(\vec{x})$ that satisfies, in vacuum, $\nabla^2\psi = 0$. (iii) When it hits the mirror (at longitudinal location $z = 0$) the incoming light beam has the Gaussian form

$$\psi = \psi_{mb}(\mathbf{y}) = \left[\frac{2I}{\lambda L}\right]^{1/4} \exp(-\pi \mathbf{y}^2/\lambda L) \tag{4.1}$$

(subscript "*mb*" for "*main beam*".) Here and throughout I is the power (energy per unit time) in the main beam, and ψ is normalized such that $|\psi|^2$ is the energy flux. The bold letter $\mathbf{y}$ denotes position in the transverse plane (a 2-vector) relative to the mirror center.

The mirror can be described by the idealized boundary condition that on its surface the field ψ must vanish. We shall describe irregularities in the mirror's surface by the surface's displacement $N(\mathbf{y})$ in the z-direction (longitudinal direction). For supermirrors it will be true that $kN \approx 2\pi N/\lambda \ll 1$. By inserting our idealized $\psi = 0$ boundary condition into the Helmholtz-Kirkhoff formula [Eq. (7) in Sec. 8.3 of Born and Wolf[4]] and expanding $e^{2ikN} = 1+2ikN$ and dropping the 1 from this expansion (since it corresponds to the perfectly reflected main beam), we obtain for the scattered field at the point P of Fig. 4.1

$$\psi(P) = \int_{\text{mirror}} \psi_{mb}\left[\frac{k^2 N}{2\pi}\right] \frac{e^{ikr}}{r} d^2\mathbf{y} \ . \tag{4.2}$$

Here the integration is over location $\mathbf{y}$ on the ideally flat mirror, $z=0$, and r is the distance from the integration point $\mathbf{y}$ to the field point P. This distance can be expressed in terms of $\mathbf{y}$, the transverse location $\mathbf{Y}$ of the field point relative to the main beam's central axis, and the longitudinal distance z of the field point from the mirror, as

$$r = [z^2+(\mathbf{Y}-\mathbf{y})^2]^{1/2} \cong z+\frac{\mathbf{Y}^2}{2z}+\frac{\mathbf{Y}}{z}\cdot\mathbf{y}+\frac{\mathbf{y}^2}{2z} \ . \tag{4.3}$$

Here terms of higher order in $1/z$ than $1/z^2$ are small compared to $\lambda/2\pi$ and thus give negligible contributions

to the phase factor in (4.2) and are omitted. By combining Eqs. (4.2) and (4.3) we obtain

$$\psi(\mathbf{Y},z) = \frac{1}{z} e^{ikz} e^{ikY^2/2z} \int_{\text{mirror}} \psi_{\text{mb}}\left(\frac{k^2 N}{2\pi}\right) e^{i(k\mathbf{Y}/z)\cdot\mathbf{y}} e^{iky^2/2z} d^2y \ . \tag{4.4}$$

The squared modulus of this field, $|\psi|^2$, is the energy flux of scattered light and thus must be equal (after spatial averaging over any fluctuations) to $z^{-2} I P_{\text{sc}}(\theta = Y/z) = z^{-2} I \alpha (z/Y)^2$. Correspondingly, we can rewrite (4.4) in the form

$$\psi(\mathbf{Y},z) = \frac{1}{z} \frac{\sqrt{\alpha I}}{Y/z} e^{ikz} e^{ikY^2/2z} f_{\text{sm}}(\mathbf{Y}) \ . \tag{4.5a}$$

Here the quantity $f_{\text{sm}}(\mathbf{Y})$ (subscript "sm" for "scattering mirror") is a complex function with rms value unity,

$$\langle f_{\text{sm}}{}^2 \rangle = 1 \ , \tag{4.5b}$$

given by

$$f_{\text{sm}}(\mathbf{Y}) = \frac{Y/z}{\sqrt{\alpha I}} \int_{\text{mirror}} \psi_{\text{mb}}\left(\frac{k^2 N}{2\pi}\right) e^{ik(\mathbf{Y}/z)\cdot\mathbf{y}} e^{-iky^2/2z} d^2y \ . \tag{4.5c}$$

In words, $f_{\text{sm}}(\mathbf{Y})$ is the fourier transform of the mirror deformation $N(\mathbf{y})$ inside the main beam's spot, evaluated at wave vector $k\mathbf{Y}/z$ and renormalized to unit rms value. If the fluctuations $N(\mathbf{y})$ in the mirror shape at transverse wave vector $k\mathbf{Y}/z$ have coherence length D_{sm}, then the Fourier transform will change substantially on scales $|k\Delta\mathbf{Y}/z| = 2\pi/D_{\text{sm}}$, i.e. on scales $|\Delta\mathbf{Y}| = 2\pi z/kD_{\text{sm}} = z\lambda/D_{\text{sm}}$. Because the fourier transform is confined to a region of radius $|\mathbf{y}| \lesssim \sqrt{\lambda L}$ by the Gaussian ψ_{mb} that appears in the integrand, the largest the coherence length D_{sm} can be in the integral is $D_{\text{max}} = \sqrt{\lambda L}$, and the smallest possible scale for variations of $f_{\text{sm}}(\mathbf{Y})$ is $|\Delta\mathbf{Y}| \gtrsim z\lambda/\sqrt{\lambda L}$); i.e.

$$f_{\text{sm}}(\mathbf{Y}) \text{ varies substantially only on scales } |\Delta\mathbf{Y}| = \frac{z\lambda}{D_{\text{sm}}} \gtrsim \frac{z}{L}\sqrt{\lambda L} \ . \tag{4.5d}$$

This lengthscale $|\Delta\mathbf{Y}|$, evaluated for the central baffles $z = L/2$, is the σ_M of Secs. III.E and IV.E.

2. Scattering of Light Back Into Main Beam

Consider, next, scattered light that is converging onto a "receiving mirror" after being reflected off the wall of the vacuum pipe and/or diffracted off a baffle. In this section we shall analyze the recombination of that light with the main beam via scattering off the receiving mirror: in the next section we shall analyze recombination via transmission through the mirror onto the photodiode: and in both sections we shall derive expressions not only for the recombination but also for the noise $\bar{i}(f)$ that results from the recombination (Sec. III.A.3). The intensity-analysis descriptions of these processes were discussed in Secs. III.A.2 and III.A.3; here we shall focus primarily on amplitude analyses.

Consider scattered light, described by the field ψ, impinging on the receiving mirror. Focus attention on the form $\psi(\mathbf{y}')$ of the incoming field at transverse location $\mathbf{y}'$ on the surface of the mirror, and also on the form $\psi_{\text{mb}}(\mathbf{y}')$ of the incoming main-beam field there. The incoming scattered field $\psi(\mathbf{y}')$ will be a superposition of locally plane waves coming from the directions of the various parts of various baffles or from various points of reflection on the vacuum-pipe wall; while $\psi(\mathbf{y}')$ will have the same Gaussian form (4.1) as on the scattering mirror, but with $\mathbf{y}$ replaced by $\mathbf{y}'$.

It can be shown, by computing the rescattering of the field $\psi(\mathbf{y}')$ via Eq. (4.2) (with ψ_{mb} replaced by ψ) and by then breaking up the rescattered field into modes of the interferometer and picking out the component

which goes into the main-beam mode, that the scattered light produces a phase change in the main beam given by

$$\delta\Phi_{mb} = \text{Imaginary}\left[\frac{1}{I}\int_{\text{mirror}} \psi^*_{mb}(\mathbf{y}')\psi(\mathbf{y}')kN(\mathbf{y}')d^2y'\right] . \tag{4.6}$$

Here $N(\mathbf{y}')$ is the displacement of the receiving mirror from ideal flatness due to irregularities, and the * denotes complex conjugation. This phase change has a time dependence produced by the modulational time dependence of the scattered field ψ; and the time-dependent portion is interpreted, upon reaching the photodiode, as associated with a gravitational-wave field

$$h(t) = \frac{\lambda}{2\pi BL}\delta\Phi_{mb} = \frac{\lambda}{2\pi BL}\text{Imaginary}\left[\frac{1}{I}\int_{\text{mirror}} \psi^*_{mb}(\mathbf{y}')\psi(\mathbf{y}',t)kN(\mathbf{y}')d^2y'\right] . \tag{4.7}$$

By expanding $\psi(\mathbf{y}',t)$ in modes of the mirror [paragraph following Eq. (4.11) below], then evaluating the spectral density of expression (4.7), assuming random relative phases of the mirror modes, and using Eqs. (4.5b,c,d), one can obtain the intensity-analysis formula (3.7), (3.5) for $\bar{h}(f)$. (This is a much harder way to get that formula than the simple argument given in Sec. III.A.)

3. Transmission of Scattered Light Onto the Photodiode

When the scattered wave ψ hits the receiving mirror, part of it gets transmitted through the mirror, along with part of the main beam, and into the photodiode. The scattered wave then, by interfering with the beam from the other arm, produces a change in the photodiode current. It can be shown that the change in phase $\delta\Phi_{mb}$ of the main beam that would have been required to produce that same change of photodiode current is

$$\delta\Phi_{mb} = \text{Imaginary}\left[\frac{1}{I}\int_{\text{mirror}} \psi^*_{mb}(\mathbf{y}')\psi(\mathbf{y}')\eta(\mathbf{y}')d^2y'\right] , \tag{4.8}$$

where the integration is over location $\mathbf{y}'$ on the corner mirror of the interferometer's arm, and $\eta(\mathbf{y}')$ is the efficiency of the photodiode for photons that move along main-beam rays passing through $\mathbf{y}'$. Notice that Eq. (4.8) is the same as (4.6), but with the mirror's deformation-produced phase shift kN replaced by the photodiode's efficiency η. Corresponding to (4.8) is the following expression for the gravitational-wave field inferred from the observed phase shift

$$h(t) = \frac{\lambda}{2\pi BL}\delta\Phi_{mb} = \frac{\lambda}{2\pi BL}\text{Imaginary}\left[\frac{1}{I}\int_{\text{mirror}} \psi^*_{mb}(\mathbf{y}')\psi(\mathbf{y}',t)\eta(\mathbf{y}')d^2y'\right] ; \tag{4.9}$$

cf. Eq. (4.7).

In concrete applications of Eq. (4.9) the scattered field ψ will arrive at the receiving mirror from some location $(z',\mathbf{Y})$ (a diffraction or scattering or reflection point on a baffle or on the vacuum-pipe wall), where z' is longitudinal distance from the plane of the receiving mirror. Then ψ evaluated on the receiving mirror will have the form $e^{i(k\mathbf{Y}/z')\cdot\mathbf{y}'}e^{iky'^2/z'}$, aside from a multiplicative factor, while ψ_{mb} will have the Gaussian form (4.1). Correspondingly, when computing the scattering-induced phase shift (4.8) we will encounter the following integral, which we shall approximate in the following way:

$$\int_{\text{mirror}} \psi_{mb}e^{i(k\mathbf{Y}/z')\cdot\mathbf{y}'}e^{iky'^2/z'}\eta d^2y' \approx \sqrt{I\lambda L}\,(1-\bar{\eta})\left(\frac{\sqrt{\lambda L}}{Y}\frac{z'}{L}\right)^{1/2} f_{pd}(\mathbf{Y}) , \tag{4.10}$$

where $f_{pd}(\mathbf{Y})$ is a fluctuating complex function with rms value of unity. In Eq. (4.10) the first term, $\sqrt{I\lambda L}$,

would be the value of the integral of ψ_{mb} alone; and the remaining part is our estimate of the integral with ψ_{mb} replaced by a normalized Gaussian (one whose integral is unity). This remaining part is essentially a Fourier transform of the photodiode efficiency, restricted to the main-beam spot. Our estimate of this Fourier transform is conservative — i.e., it is more likely an overestimate than an underestimate. The magnitude of our estimate, $(1-\bar{\eta})[(\sqrt{\lambda L}/Y)z'/L]^{1/2}$, is the mean deviation of the efficiency from unity, divided by the square root of the number of half-waves of $e^{i(kY/z')Y'}$ contained in the integration region. The function $f_{pd}(Y)$ describes the fluctuations in this Fourier transform, which are caused by the random fluctuations in the photodiode efficiency. By analogy with Eq. (4.5d),

$$f_{pd}(Y) \text{ varies substantially only on scales } |\Delta Y| = \frac{z'\lambda}{D_{pd}} \geq \frac{z'}{L}\sqrt{\lambda L} \ , \tag{4.11}$$

where $D_{pd} \leq \sqrt{\lambda L}$ is the coherence length for fluctuations of η at transverse wave vector $\varkappa = kY/z'$ within the main-beam spot. This $|\Delta Y|$, evaluated for the central baffles $z' = L/2$, is the σ_{pd} of Secs. III.E and IV.E.

Equations (4.8)—(4.11) constitute our highest-accuracy description of the effects of direct propagation of scattered light into the photodiode. In this description no assumptions are made about the phase coherence of the scattered light. To see that phase coherence typically will not be important here or in the case of recombination via scattering (preceding section), consider the incoming scattered field $\psi(y')$ evaluated on the receiving mirror. That field can be written as a sum over modes of the mirror (solutions to the two-dimensional Laplace equation) that are restricted to the interior of the Gaussian beam spot — or, for greater conceptual simplicity, restricted to the interior of a square of side $\sqrt{\lambda L}$. Then the Cartesian components of the transverse wave vectors $\varkappa$ of these mirror modes will be multiples of $2\pi/\sqrt{\lambda L}$; and correspondingly, the region in transverse wave-vector space occupied by each mode will have linear size $|\Delta\varkappa| = 2\pi/\sqrt{\lambda L}$. Equation (4.10) shows that the transverse wave vector is related to the location (z',Y) from which the scattered light comes by $\varkappa = k(Y/z') = 2\pi Y/\lambda z'$; and correspondingly, regions of transverse size $|\Delta Y| = z'\lambda/\sqrt{\lambda L} = (z'/L)\sqrt{\lambda L}$ all contribute to a single mirror mode of ψ. This means that, if the lengthscale for phase fluctuations in the scattered light at z' is $|\Delta Y| \leq (z'/L)\sqrt{\lambda L}$, then the various mirror modes in ψ will have random phases relative to each other and thus will contribute incoherently to the integral (4.8). In fact, the lengthscale for such phase fluctuations typically (but not always) *will* be $\lesssim (z'/L)\sqrt{\lambda L}$ because the light from the original scattering mirror is likely to have lengthscales not much larger than this [cf. Eq. (4.5d)], the photodiode response [Eq. (4.11)] is likely to be characterized by lengthscales not much larger than this, and interactions with baffles and the pipe wall are likely to further randomize the phases. This justifies our extensive use of intensity-analysis techniques in this report. For a more detailed discussion of the effects of phase coherence and of situations in which the intensity analysis may break down, see Sec. IV.E below.

Returning to our analysis of scattered light impinging on the photodiode, we next shall rewrite ψ in Eq. (4.9) as a sum over modes and use (4.10) to evaluate each mode's contribution to the integral. Thereby we obtain

$$h(t) = \frac{\lambda}{2\pi BL}\text{Imaginary}\left[\frac{1}{I}\sum_{\varkappa}\sqrt{(dE/dA)_{\varkappa}}\exp(i\Phi_{\varkappa})\sqrt{I\lambda L}\,(1-\bar{\eta})\left(\frac{\sqrt{\lambda L}}{L}\frac{1}{\theta}\right)^{1/2}\right] . \tag{4.12}$$

Here θ is the angle to the main beam at which a given mode's photons come in, and $\Phi_{\varkappa}$ is the phase of the contribution from mode $\varkappa$. The square root of the spectral density of this $h(t)$, when the relative phases of the various modes are random, is

$$\tilde{h}(f) = \frac{1}{2\pi BL}(1-\bar{\eta})\left[\frac{1}{2}\sum_{\varkappa}\frac{(dE/dAdf)_{\varkappa}}{I/\lambda L}\left(\frac{\lambda}{L}\right)^{1/2}\frac{1}{\theta}\right]^{1/2} . \tag{4.13}$$

Converting the sum over modes to an integral over directions of the incoming scattered light, and comparing

the resulting expression to the standard one (3.7), we can read off the value of the "recombination probability" for scattered light transmitted to the photodiode:

$$P_{\text{rec}}(\theta) = \frac{(1-\bar{\eta})^2}{2\theta}\left[\frac{\lambda}{L}\right]^{1/2} . \tag{4.14}$$

This is the expression quoted without full proof in Eq. (3.6).

4. Frequency Modulation of Light by Reflection off the Pipe Walls and Diffraction and Scattering off Baffles

Turn next to a derivation of expression (3.8) for the frequency modulation of light that gets reflected off the pipe walls.

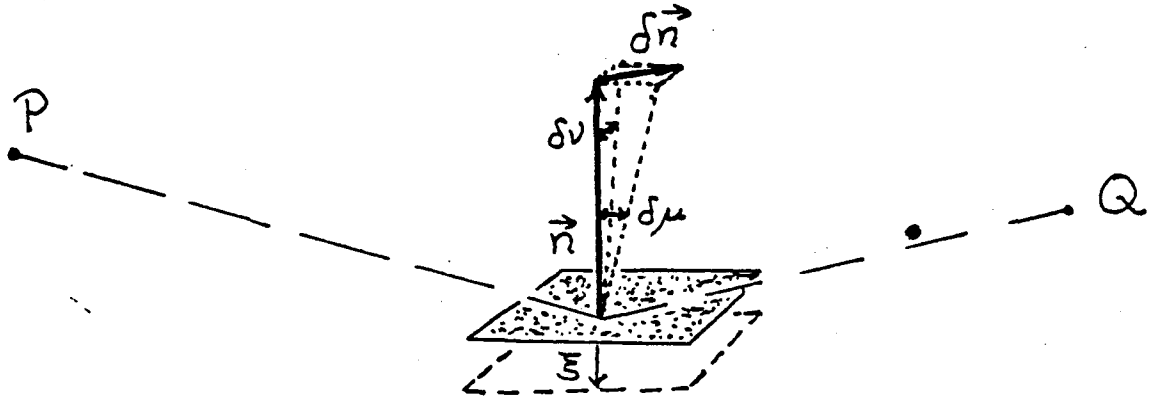

Fig. 4.2 The geometry of a ray from point P to point Q which is reflected in a locally flat portion of the vacuum pipe's wall. Motion-induced changes in the wall are described by the normal displacement ξ at the point of reflection and by angular displacements $\delta\mu$ and $\delta\nu$ of the normal $\vec{n}$ at the point of reflection.

Consider, as a first step in the derivation, an idealized problem in which light propagates from one point P to another point Q via small-angle reflection in the wall (Fig. 4.2). If the wall's geometry fluctuates relative to P and Q, how will the length r of the reflecting ray from P to Q change? The geometric fluctuations can be split up into a displacement ξ of the wall normal to itself at the point of reflection, plus a change $\delta\vec{n}$ in the direction of the normal $\vec{n}$. The change of $\vec{n}$ is described by two angles. The first, $\delta\mu$ is the angle of the new $\vec{n}$ to the old one, projected into the plane of the original ray; this is also describable as the change of the angle μ of inclination of the line PQ to the wall. The second angle, $\delta\nu$, is the change of $\vec{n}$ projected on the plane perpendicular to the original ray. It is easy to convince oneself that $\delta\nu$ has no first-order effect on the length r of the ray from P to Q. However, as one readily sees from the diagrams in Fig. 4.3, both the displacement ξ and the angle $\delta\mu$ do have first-order influences δr; and they, and the corresponding changes $\delta\Phi = 2\pi\delta r/\lambda$ in the phase of light that propagates from P to Q, are given by the following equations:

$$\delta\Phi = 2\pi\frac{\delta r}{\lambda} = \frac{4\pi}{\lambda}(a+b)\frac{\xi}{c} . \tag{4.15a}$$

and

$$\delta\Phi = 2\pi\frac{\delta r}{\lambda} = \frac{4\pi}{\lambda}(b-a)\delta\mu . \tag{4.15b}$$

Here a, b, and c are the distances shown in Fig. 4.3.

Turn, next, to the slightly more realistic (but not fully realistic) problem of light that scatters off one mirror and travels to the other via a series of reflections in the pipe wall (but no diffractions or scatterings);

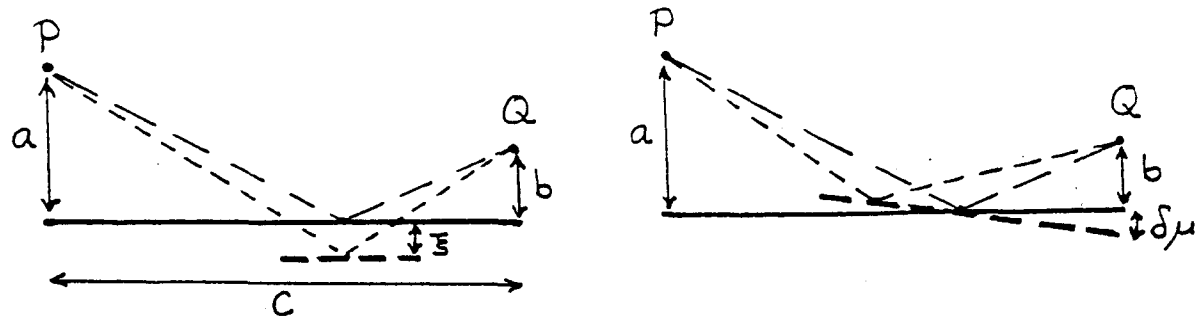

Fig. 4.3 Geometry for computing the changes of the length of the ray from P to Q induced by the displacement ξ and tilt $\delta\mu$ of the wall.

and restrict attention for simplicity to the case of a ray whose transverse motion is radial (i.e. which passes repeatedly through the central axis of the vacuum pipe). In this case, if l is the distance from the scattering mirror to a specific reflection point and θ is the angle of the ray relative to the main beam and the pipe axis and $\bar{\mu}$ is the angle of the unperturbed wall to the unperturbed main beam, and if for conceptual ease we imagine straightening out the ray at all reflection points except the one being studied, then the lengths $a+b$, $b-a$ and c of Figs. 4.2 and 4.3 becomes

$$a+b = L\theta + L\sigma_{\bar{\mu}}\sqrt{L\theta/2R}\ , \quad b-a = (2L-l)\theta + L\sigma_{\bar{\mu}}\sqrt{L\theta/2R}\ , \quad c = L\ . \tag{4.16}$$

Here $L\sigma_{\bar{\mu}}\sqrt{L\theta/2R}$ is an estimate of the stochastic effects of the time-averaged wall angles $\bar{\mu}$ at all $N_{\rm ref} = L\theta/2R$ reflection points along the route from one mirror to the other. This may be an overestimate when θ is large, because of anticorrelations in $\bar{\mu}$ from one segment of pipe to another; but when θ is large the $L\theta$ and $(2L-l)\theta$ terms dominate, so the error in the estimate $L\sigma_{\bar{\mu}}\sqrt{L\theta/2R}$ is unimportant. Corresponding to the values (4.16) of $a+b$, $b-a$, and c are the following expressions for the changes of phase (4.15a,b):

$$\delta\Phi = 4\pi(\theta + \sqrt{L\theta/2R}\ \sigma_{\bar{\mu}})\frac{\xi}{\lambda}\ , \tag{4.17a}$$

$$\delta\Phi = 4\pi\left[\frac{(L-2l)\theta + L\sqrt{L\theta/2R}\ \sigma_{\bar{\mu}}}{\lambda}\right]\delta\mu\ . \tag{4.17b}$$

The phase shift will still be given by (4.17) to within a factor of order unity in the more realistic cases of rays whose whose transverse motions are not radial, and rays that interact with baffles before and/or after the reflection — so long as the baffles are near the ends of the pipe. Moreover, in all these cases the modulation put onto the light by fluctuations in the phase shift is given by the standard formula

$$\Delta\frac{dE}{dtdAdf} = \frac{dE}{dtdA}\tilde{\Phi}^2(f)\ , \tag{4.18}$$

where $\tilde{\Phi}^2(f)$ is the spectral density of $\delta\Phi(t)$.

The wall motion will be characterized by sound waves with propagation speed roughly 2×10^4 cm/sec and thus with wavelength $\lambda_{\rm sound} \sim (2000\ {\rm cm})(10\ {\rm Hz}/f)$ and with $\bar{\mu} \sim 2\pi\xi/\lambda_{\rm sound}$. Correspondingly, the ratio of $\delta\mu$-induced phase shift to ξ-induced phase shift will be

$$\frac{\delta\Phi_{\delta\mu}}{\delta\Phi_{\xi}} \sim \frac{2\pi L}{\lambda_{\rm sound}} \gg 1\ ; \tag{4.19}$$

which means that we can (and shall) ignore the ξ-induced phase shift compared to the $\delta\mu$-induced shift when dealing with light that reflects off the pipe walls.

When light diffracts off a baffle the only contributor to phase and frequency modulation is the baffle's vertical displacement ξ. It is easy to show that, by analogy with Eq. (4.17a)

$$\delta\Phi = 2\pi(\theta+\theta')\frac{\xi}{\lambda}\,, \tag{4.20}$$

where θ is the angle of the incoming light and θ' is the angle of the outgoing light. By combining this with Eq. (4.18) we obtain expression (3.12) for the diffraction-induced change in the specific flux of frequency-modulated light.

In the case of scattering off a baffle (Sec. III.A.7), it is the longitudinal displacement ξ of the baffle that produces the phase shift; and one easily sees that the shift is $\delta\Phi = 4\pi\xi/\lambda$ corresponding to Eq. (3.20) for the production of frequency-modulated light.

5. Diffraction off Baffles

Turn, next, to diffraction of light off a baffle. For ease of analysis, approximate the baffle as plane parallel rather than cylindrical. This is justified by the fact that, unless the mirrors are very near the pipe center (a case treated separately in Sec. IV.E), the scattered light's transverse lengthscales (coherence lengthscale and lengthscale of Fresnel diffraction pattern) are small compared to the baffle's radius of curvature. Let the baffle be jagged, with height variations $H(x)$ where x is distance along the baffle. Denote by y vertical distance measured from the mean baffle top and by z longitudinal distance away from the baffle; see Fig. 4.4.

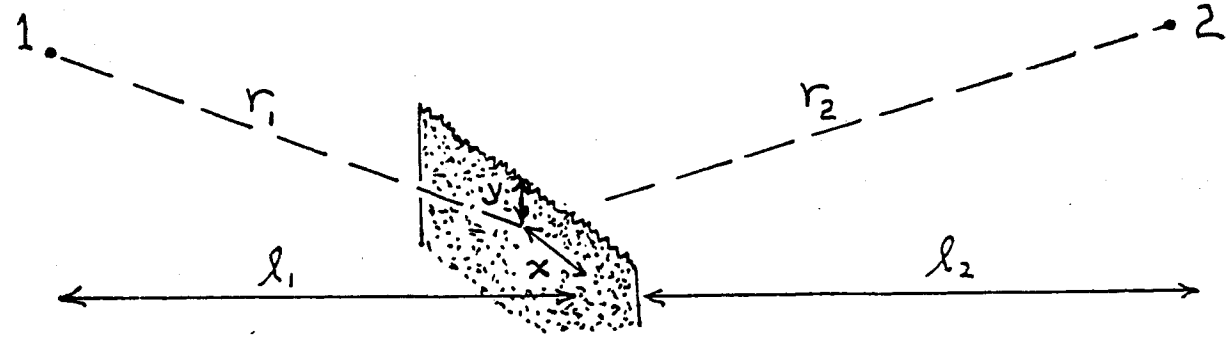

Fig. 4.4 Geometry for derivation of the diffraction cross section and for discussion of its dependence on jaggedness of the edge of a baffle.

Place a point source of light, with outgoing field $\psi = e^{ikr}/r$, at location $(z_1 = -l_1, y_1 = \theta_1 l_1, x_1)$; and examine the diffracted field at location $(z_2 = l_2, y_2 = \theta_2 l_2, x_2)$. By definition, the diffracted field is the difference between the field that would exist at point 2 in the absence of the baffle and that in the presence of the baffle; and by Babinet's Principle (Born and Wolf[4] p. 381) and the Fresnel-Kirchoff diffraction formula (Born and Wolf[4] p. 382) this field can be expressed as the following integral over the region covered by the baffle:

$$\psi = \frac{-i}{\lambda l_1 l_2}\int_{-\infty}^{+\infty} dx \int_{-\infty}^{H} dy\; e^{ik(r_1+r_2)}\,. \tag{4.21}$$

A little geometry and algebra permit one to write r_1+r_2 in the form

$$r_1+r_2 = l_1+l_2+\frac{(x-x_1-x_2)^2}{2l_R}+\frac{[y-(\theta_1+\theta_2)l_R]^2}{2l_R}+\frac{(\theta_1 l_1-\theta_2 l_2)^2}{2(l_1+l_2)}+\frac{(x_1-x_2)^2}{2(l_1+l_2)}\,. \tag{4.22}$$

Here l_R is the reduced length of the baffle from the source and field points, $l_R \equiv l_1 l_2/(l_1+l_2)$. By inserting expression (4.22) into (4.21) and evaluating the y integral using the approximation, valid for $\omega \gg 1$,

$$\int_{\omega}^{\infty} e^{(i\pi/2)\tau^2} d\tau \equiv \frac{i}{\pi\omega} e^{(i\pi/2)\omega^2}, \tag{4.23}$$

we obtain

$$\psi = \frac{e^{i\Phi_o}}{2\pi l_1 l_2} \frac{1}{(\theta_1+\theta_2)} \int_{-\infty}^{+\infty} dx \exp\left[\frac{i\pi(x-x_1-x_2)^2}{\lambda l_R}\right] W(x), \tag{4.24}$$

where Φ_o is a phase that we shall not write down and $W(x)$ is unity if the baffles are smooth, and is the complex random function

$$W = e^{-ik(\theta_1+\theta_2)H(x)} \tag{4.25}$$

if the baffles are randomly jagged. The strategy of jagged baffles would dictate that $H(x)$ vary with a sufficiently large amplitude to make the phase of W change by π on some short lengthscale σ_H. In this case we can regard expression (4.24) as a filter of the "random process" $W(x)$. The input to this filter is the function $W(x)$ of position x on the baffle; the output is a function of the lateral position x_2 of the observation point. The output fluctuates randomly with changing x_2. We are interested not in the details of those fluctuations, but instead in the rms value of the output ψ averaged over x_2. We can estimate that rms value as follows:

If the real and imaginary parts of W ($W_R = \cos[ik(\theta_1+\theta_2)H(x)]$ and $W_I = -\sin[ik(\theta_1+\theta_2)H(x)]$) were uncorrelated, then $\psi(x_2)$ [Eq. (4.24)] would have the same rms value as the "modified" ψ

$$\psi_{\text{mod}} = \frac{1}{2\pi l_1 l_2} \frac{1}{(\theta_1+\theta_2)} J(x_2), \tag{4.26a}$$

where

$$J(x_2) \equiv 2\int_{-\infty}^{+\infty} \cos\left[\frac{i\pi(x-x_2)^2}{\lambda l_R}\right] W_R(x)\,dx. \tag{4.26b}$$

The correlation between W_R and W_I will not alter the equality of $|\psi|_{\text{rms}}$ and $|\psi_{\text{mod}}|_{\text{rms}}$ by more than $\sim\sqrt{2}$. Then the modulus of the Fourier transform of the filter $K(\xi) \equiv 2\cos[i\pi\xi^2/\lambda l_R]$, which appears in (4.26b), is

$$|\tilde{K}(f)|^2 = 2\lambda l_R[1+\sin(2\pi\lambda l_R f^2)]; \tag{4.27}$$

and correspondingly, if $S_{W_R}(f)$ is the spectral density of $W_R(x)$, then the spectral density of $J(x_2)$ is $S_J(f) = |\tilde{K}(f)|^2 S_{W_R}(f)$; and rms value of J is

$$J_{\text{rms}} = \left[2\lambda l_R \int_0^{+\infty} [1+\sin(2\pi\lambda l_R f^2)] S_{W_R}(f)\,df\right]^{1/2} \tag{4.28}$$

Figure 4.5 shows the two components of the integrand, $S_{W_R}(f)$ and $1+\sin(2\pi\lambda l_R f^2)$ for two extreme cases: (a) lengthscale σ_H on which the baffle height varies (and hence on which $W_R(x)$ varies) large compared to $\sqrt{\lambda l_R}$ = (the transverse size of the largest Fresnel zone on the baffle's edge); and (b) $\sigma_H \ll \sqrt{\lambda l_R}$. It should be evident from the figure that the value of the integral (4.28) is the same in the two domains: *The rms value of J and thence of ψ is independent of the lengthscale σ_H on which the baffle height varies; for all σ_H, to within a factor of order 2, $|\psi|_{\text{rms}}$ is equal to the value for a completely smooth baffle.*

$$|\psi|^2_{\text{rms}} = \frac{1}{4\pi^2(l_1+l_2)^2} \frac{\lambda/l_R}{(\theta_1+\theta_2)^2}. \tag{4.29}$$

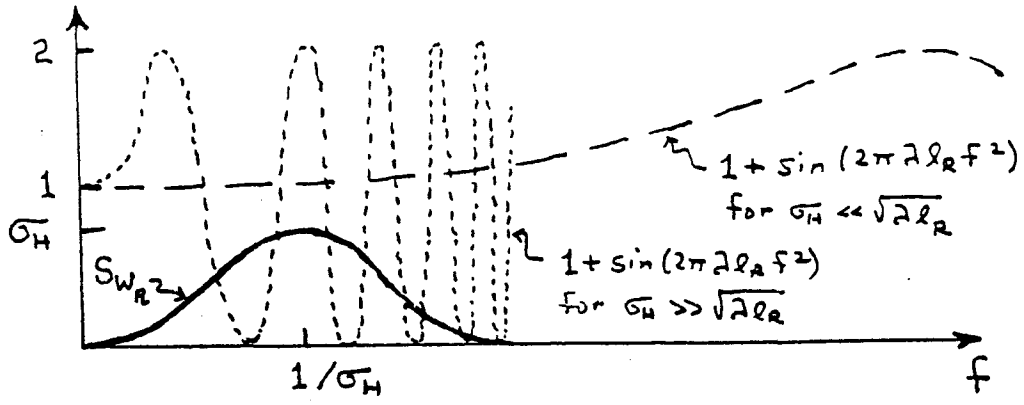

Fig. 4.5 Components of the integrand (4.28).

Thus, the baffle jaggedness does not change the diffracted light's intensity distribution.

This conclusion can be understood in the following way: *When the baffle is smooth* the contribution to ψ from each Fresnel zone on the baffle is relatively large, but the contributions from adjacent Fresnel zones cancel each other almost perfectly, in the manner of a Cornu spiral. As a result, essentially all of the contribution to $|\psi|^2_{\rm rms}$ comes from the central Fresnel zone [$|x-x_1-x_2| \lesssim \sqrt{\lambda l_R}$ in Eq. (4.24)]. Note that this zone has about the right size to contribute to only one or a few modes of the receiving mirror [paragraph following Eq. (4.11)], thereby guaranteeing that phase coherence will be fairly unimportant when the scattered light diffracts off a smooth baffle. *When the baffle is jagged* on a short lengthscale $\sigma_H \ll \sqrt{\lambda l_R}$, this jaggedness reduces by a large factor the contribution of each Fresnel zone to ψ, but it also spoils the delicate cancellation between the contributions of adjacent Fresnel zones. The two effects compensate, and the rms value of ψ is unchanged. However, the field ψ now comes from a region on the jagged baffle with transverse size $\Delta x = \lambda l_R/\sigma_H \gg \sqrt{\lambda l_R}$. This means the baffle feeds many modes of the receiving mirror — a situation that would cause danger from phase coherence were it not for the randomization of phases produced by the jaggedness itself.

The bottom line is that (when the mirrors are not very near the pipe's center) *jaggedness is unimportant: It neither influences the cross section nor disturbs the insensitivity to phase coherence.*

From the diffracted field (4.29) we can compute the cross section $d\sigma/dx d\theta_2$ for diffraction: The energy flux incident on the baffle is $(dE/dAdt)_{\rm in} = 1/l_1^2$, and the total energy diffracted by a length Δx of baffle into a range $\Delta\theta_2$ of θ_2 is $(dE/dt)_{\rm diff} = |\psi|^2[\Delta x(l_1+l_2)/l_1]\Delta\theta_2 l_2$; and correspondingly [cf. the definition (3.9) of the cross section, with the change of notation $\theta_1 = \theta$ and $\theta_2 = \theta'$]

$$\frac{d\sigma}{dx d\theta_2} = \frac{(dE/dt)_{\rm diff}}{(dE/dtdA)_{\rm in}\Delta x\,\Delta\theta_2} = l_1 l_2(l_1+l_2)|\psi|^2 = \frac{\lambda}{4\pi^2(\theta_1+\theta_2)^2} . \tag{4.30}$$

This is the cross section quoted in Eq. (3.10).

6. Diffraction-Aided Reflection

Turn attention, finally, to diffraction-aided reflection. As in the above study of ordinary diffraction, we shall compute the diffracted/reflected field and the resulting cross section using a plane parallel approximation. For simplicity we shall presume that the baffles are smooth rather than jagged. The geometry of the calculation is shown in Fig. 4.6.

We presume that the field emitted from point 1 has the form, near point 1, $\psi = e^{ikr}/r$; and we denote by $\theta_1 \equiv (Y_1-H_1)/l_1$ the light's incident angle, by $\theta_2 = (Y_2-H_2)/l_2$ its outgoing angle, and by $\theta_n \equiv (H_1+H_2)/s$ the

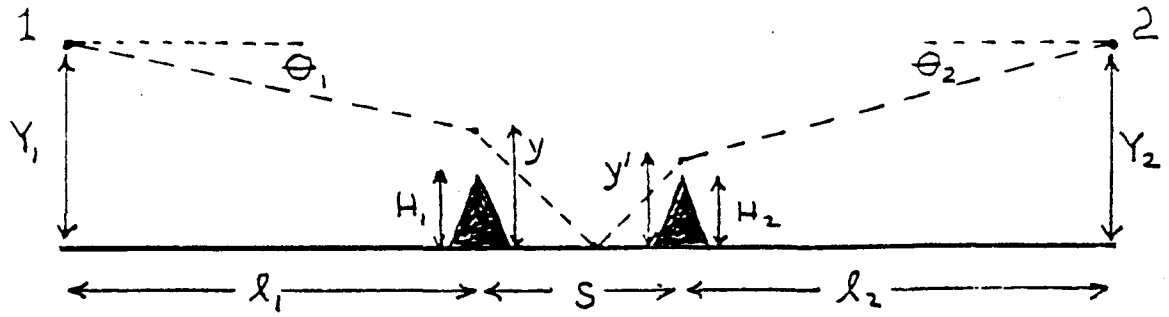

Fig. 4.6 Geometry for derivation of the cross section for diffraction-aided reflection. The field at point 2 is written, in Eqs. (4.31), as a sum over all paths of propagation with the form shown dotted in this diagram. The transverse, x-direction is suppressed from the diagram.

minimum incoming angle the light would have to have in order to escape the baffles. (In this section, and only here, transverse distances Y are measured to the pipe wall rather than to the smoothed baffle tops.) We further denote $L = l_1+s+l_2$ and $l_R = l_1 l_2/L$, and we restrict attention to the regime

$$\theta_n - \theta_1 \gg \left[\frac{\lambda}{4\pi^2 s}\right]^{1/3}, \quad s \ll l_1, \quad s \ll l_2. \tag{4.31}$$

Then by a double application of the Fresnel-Kirchoff diffraction formula [a sum over all possible paths of the form shown dotted in Fig. 4.6 — paths involving propagation from the source point to an arbitrary point (x,y) in the plane of the first baffle, then a bend of the ray downward, then propagation via specular reflection off the mirror to the plane of the second baffle, then a bend of the ray, then propagation to point 2], we can write the field at point 2 as

$$\psi = -\frac{e^{ikL}}{\lambda^2 l_1 s l_2} I_x I_y, \tag{4.32a}$$

where

$$I_x = \int_{-\infty}^{+\infty}\int_{-\infty}^{+\infty} \exp\left[\frac{ik}{2}\left(\frac{x^2}{l_1}+\frac{(x-x')^2}{s}+\frac{x'^2}{l_2}\right)\right] dx\,dx' = i\lambda\left[\frac{l_1 s l_2}{L}\right]^{1/2}, \tag{4.32b}$$

$$I_y = \int_{H_1}^{\infty} dy \int_{H_1}^{\infty} dy' \exp\left[\frac{ik}{2}\left(\frac{(Y_1-y')^2}{l_1}+\frac{(y'+y)^2}{s}+\frac{(Y_2-y)^2}{l_2}\right)\right]$$

$$= \int_0^{+\infty} d\xi \int_0^{+\infty} d\xi' \exp\left[\frac{ik}{2}\left(\frac{(\xi'-l_1\theta_1)^2}{l_1}+\frac{(\xi'+\xi+s\,\theta_o)^2}{s}+\frac{(\xi-l_2\theta_2)^2}{l_2}\right)\right]. \tag{4.32c}$$

The ξ' integral can be expressed in terms of the Fresnel-integral function

$$F(\omega) = C(\omega)+iS(\omega) = \int_0^{\infty} e^{(i\pi/2)\tau^2} d\tau \tag{4.33a}$$

$$\equiv \omega \quad \text{for } |\omega| \ll 1, \tag{4.33b}$$

$$\equiv \frac{1+i}{2} - \frac{i}{\pi\omega} e^{(i\pi/2)\omega^2} \quad \text{for } \omega \gg 1, \tag{4.33c}$$

$$\cong -\frac{1+i}{2} - \frac{i}{\pi\omega} e^{(i\pi/2)\omega^2} \quad \text{for } \omega \ll -1 \,. \tag{4.33d}$$

By doing so, by invoking (4.31), and by making use of the approximations (4.33c) and $s/l_2 \ll 1$ and setting $k = 2\pi/\lambda$, we obtain

$$I_y = \frac{\lambda}{2\pi} e^{i\Phi_o} \int_0^\infty \frac{d\xi}{\theta_n - \theta_1 + \xi/s} \exp\left[\frac{i\pi}{\lambda}[\xi + (\theta_n - \theta_2)s]^2\right]$$

$$= \frac{\lambda}{2\pi}\left(\frac{s\lambda}{2}\right)^{1/2} e^{i\Phi_o} \int_{-\sqrt{(2s/\lambda)}(\theta_2-\theta_n)}^{\infty} \frac{e^{(i\pi/2)\tau^2}}{\theta_2 - \theta_1 + \sqrt{\lambda/2s}\,\tau} d\tau \,, \tag{4.33}$$

where Φ_o is a phase that we shall not bother to write down. In the regime $\theta_2 - \theta_n \ll -\sqrt{\lambda/4\pi^2 s}$ the integral begins at $\tau \gg 1$ and goes to $+\infty$. The dominant contribution to the integral then comes from near the lower limit; and, accordingly, the slowly changing denominator can be evaluated there. By doing so we convert the integral into the form (4.33a) of a Fresnel-integral function, which can then be approximated by (4.33c) giving

$$I_y = \frac{\lambda^2}{4\pi^2} \frac{e^{i\Phi_1}}{(\theta_n - \theta_1)(\theta_n - \theta_2)} \quad \text{for } \theta_2 - \theta_n \ll -\sqrt{\lambda/4\pi^2 s} \,. \tag{4.34}$$

Here Φ_1 is a phase that we shall not write down. In the regime $\theta_2 - \theta_n \gg +\sqrt{\lambda/4\pi^2 s}$ the integral begins at $\tau \ll -1$ and goes to $+\infty$. The dominant contribution to the integral then comes from $\tau = 0$; and accordingly the slowly changing denominator can be evaluated there. By doing so and using the approximate value $1+i$ for the resulting Fresnel integral, we obtain

$$I_y = \frac{\lambda}{2\pi} \frac{\sqrt{\lambda s}}{\theta_2 - \theta_1} e^{i\Phi_2} \quad \text{for } \theta_2 - \theta_n \gg +\sqrt{\lambda/4\pi^2 s} \,. \tag{4.35}$$

Here Φ_2 is a phase that we shall not write down. By combining Eqs. (4.32a,b), (4.34), and (4.35) we obtain the diffracted/reflected field ψ. By inserting this field into $d\sigma/dx d\theta_2 = l_1 l_2 L\,|\psi|^2$ [Eq. (4.30) above] and by making the change of notation $\theta_1 = \theta$, $\theta_2 = \theta'$, $l_1 = l_n$, $l_2 = L - l_n$, $l_R = l_{Rn}$, $s = s_n$, we obtain expression (3.15) for the cross section to produce diffracted/reflected light.

By noting that the expression (4.32) for the diffracted/reflected field ψ [which is always valid, even when (4.31) is violated] is symmetric under integchange of the pair (θ_1, l_1) with the pair (θ_2, l_2) and by feeding this fact into the expression $d\sigma/dx d\theta_2 = l_1 l_2 L\,|\psi|^2$, we infer that the cross section $d\sigma/dx d\theta_2$ is also always symmetric under interchange of these pairs.

The above calculation also produces, for the phase of the diffracted-reflected light in the regime $\theta_1 > \theta_n$ and in the notation of this section

$$\Phi = \frac{\pi}{2\lambda}\left[s\left(\frac{l_1\theta_1 + l_2\theta_2}{l_1 + l_2}\right)^2 + \frac{(l_1\theta_1 + l_2\theta_2)^2}{l_1 + l_2}\right] = \frac{\pi}{2\lambda}\frac{(l_1\theta_1 + l_2\theta_2)^2}{l_1 + l_2} \tag{4.36}$$

When the wall moves radially by an amount ξ, the quantities $l_1\theta_1$ and $l_2\theta_2$ both change by ξ and correspondingly the phase of the scattered light changes by

$$\delta\Phi = -\pi \frac{l_1\theta_1 + l_2\theta_2}{\lambda}\frac{\xi}{L} = -\pi\theta_1 \frac{\xi}{\lambda} \,. \tag{4.37a}$$

When the longitudinal slope of the wall changes by $\delta\mu$, the incident and diffracted angles change by $\delta\theta_1 = \mu$ and $\delta\theta_2 = -\mu$, and the corresponding phase change is

$$\delta\Phi = \pi \frac{l_1\theta_1 + l_2\theta_2}{\lambda}\left(\frac{l_1 - l_2}{L}\right)\delta\mu = \pi\theta_1\left(\frac{l_1 - l_2}{\lambda}\right)\delta\mu \,. \tag{4.37b}$$

By the same estimate as we used in discussing reflected light [Eq. (4.19)] it is seen that the $\delta\mu$-induced phase change will almost always be larger than the ξ-induced phase change. Correspondingly, the phase modulation put onto the scattered light by diffraction-aided reflection is

$$\Delta\frac{dE}{dtdAdf} = \frac{dE}{dtdA}\tilde{\Phi}^2(f) = \frac{dE}{dtdA}\left[\pi\theta_1\left(\frac{l_1-l_2}{\lambda}\right)\tilde{\mu}\right]^2 . \tag{4.38}$$

This is the relation (3.18) quoted in Sec. III.A.7.

B. LIGO with No Baffles

Turn, next, to the use of these results to derive the scattering formulas of Sec. III.

Consider, first, a LIGO without baffles. In such a LIGO the dominant scattering noise would be due to the process depicted in Fig. 3.4: Light scatters off one mirror at an angle $\theta < \theta_o$, then propagates down the pipe making $N_{\rm ref}(\theta) = L\theta/2R$ reflections and getting frequency modulated at each reflection, then reaches the other mirror where it recombines with the main beam.

We shall compute the noise due to this process using Eq. (3.7), modified so the integration is over the scattering angle θ rather than over solid angle Ω:

$$\tilde{h}(f) = \frac{\lambda}{2\pi BL}\left[\int_{2R/L}^{\theta_o} P_{\rm rec}(\theta)\frac{dE_{\rm sc}/dtdAd\theta df}{I/\lambda L}d\theta\right]^{1/2} . \tag{4.39}$$

This approach is motivated by the fact that the angle θ is conserved along each reflecting photon's trajectory.

At the reflection which occurs at a distance l from the scattering mirror, static irregularities of magnitude σ_{μ_o} in the wall angle influence a photon's subsequent direction, changing the transverse location of its arrival at the plane of the receiving mirror by a distance $\delta Y \sim \sigma_{\mu_o}(L-l)$. Because of the recommended minimum in the wall irregularities, $\sigma_{\mu_o} > 10^{-4}$, this random change in the arrival location is $\delta Y \gtrsim 50\,{\rm cm}\,(1-l/L)$, which is of order the pipe's radius. It will turn out that the largest angles, $\theta \sim \theta_o$, which have the largest number of reflections, $N_{\rm ref} \sim L\theta_o/2R \sim 300(\theta_o/0.1)$, dominate the integral (4.39); and correspondingly, each photon experiences a huge number of random $\gtrsim 50\,{\rm cm}$ perturbations to its arrival location. As a result, the light from the scattering mirror gets smeared out in the plane of the receiving mirror in a rather uniform way. This permits us to write the specific intensity of the light arriving at the receiving mirror in the form

$$\frac{dE_{\rm sc}}{dtdAd\theta df} = \frac{1}{\pi R^2}\frac{dE_{\rm sc}}{dtd\theta df} . \tag{4.40}$$

The quantity $dE_{\rm sc}/dtd\theta df$ can be written in turn as

$$\frac{dE_{\rm sc}}{dtd\theta df} = \frac{dE_{\rm sc}}{dtd\theta}\tilde{\Phi}^2 , \tag{4.41}$$

where $dE_{\rm sc}/dtd\theta$ is the power scattered into a unit angle at the scattering mirror,

$$\frac{dE_{\rm sc}}{dtd\theta} = \frac{\alpha}{\theta^2}I\frac{d\Omega}{d\theta} = \frac{2\pi\alpha I}{\theta} . \tag{4.42}$$

[cf. Eqs. (3.3) and (3.4)] and $\tilde{\Phi}^2$ is the total phase modulation put onto the light in all its reflections

$$\tilde{\Phi}^2 = \sum_{j=1}^{N_{\rm ref}}\left[4\pi\frac{[L-2jL/(N_{\rm ref}+1)]\theta}{\lambda}\tilde{\mu}\right]^2 , \quad \text{with } N_{\rm ref} = L\theta/2R \tag{4.43}$$

[cf. Eq. (3.8) with the σ_{μ_n} omitted because in this case, where large angles $\theta \sim \theta_o$ dominate, its contribution is negligible]. By (i) performing the sum in (4.43) to get

$$\tilde{\Phi}^2 = \frac{1}{3}\left(\frac{4\pi L}{\lambda}\right)^2 \frac{L}{2R}\theta^3 \tilde{\mu}^2 , \tag{4.43'}$$

then (ii) combining Eqs. (4.40)—(4.43) to get $dE_{sc}/dtdAd\theta df$, then (iii) inserting this and expressions (3.5) and (3.6) for $P_{rec}(\theta)$ into Eq. (4.39), and then performing the integral, we obtain the final results for $\tilde{h}(f)$ that were quoted and discussed in Sec. III.B: Eqs. (3.21) and (3.23).

C. LIGO With Baffles: Diffraction-Aided Reflection

When baffles are included in the LIGO the dominant scattering noise is that depicted in Fig. 3.5: Photons scatter off a mirror, circumvent the first pair of baffles they encounter by a diffraction-aided reflection, then reflect their way down to the other end of the pipe where (i) if there is no second set of baffles they simply encounter the second mirror and recombine there with the main beam, or (ii) if there is a second set of baffles they undergo a final diffraction-aided reflection before recombining.

The calculation of the noise from this process follows the same pattern as the calculation for no baffles (Sec. IV.B, above). The only difference is the need to include the effects of the diffraction-aided reflection.

The largest noise occurs when the mirrors are close to the wall of the vacuum pipe, because it then is easiest for the photons to undergo the diffraction-aided reflection. We shall restrict attention to this case. Those photons which emerge from the scattering mirror propagating toward the nearby wall get stopped with great efficiency, so we shall ignore them. For those which emerge propagating toward the far wall and there encounter the baffle pair n, $n+1$, the angle θ_n appearing in the cross section for diffraction-aided reflection is given by Eq. (3.14) with the $\geq$ replaced by $=$:

$$\theta_n = \theta(1+\delta H/H) . \tag{4.44}$$

(Here and throughout we make the approximation that the baffles' height-safety factor δH is small compared to their height H, and we linearize in $\delta H/H$. We also ignore the first series of uniformly spaced baffles. The first photon with $\theta \geq \theta_o$ from our chosen mirror hits its first baffle pair only at the end of the uniformly spaced series.)

The diffraction-aided reflection boosts the photons from angle θ to

$$\theta' = \theta_n + (\text{several})\times(\theta_n - \theta) = \theta(1+3\delta H/H) . \tag{4.45}$$

For comparison, because the critical angle θ_n is decreasing along the pipe at the rate $d\theta_n/dl_n = \theta_n/l_n$, the second pair of baffles encountered by the diffracted-reflected photons (twice as far down the pipe as the first pair) has $\theta_{n'} = \theta_n/2$; and thus this second pair is easily surmounted using an ordinary reflection.

The total cross section, per unit length of baffle, for the diffraction-aided reflection is, by Eqs. (3.17) and (4.44),

$$\frac{d\sigma}{dx} = \frac{1}{4\pi^2}\frac{H}{\delta H}\frac{\lambda}{\theta} \tag{4.46}$$

The energy flux hitting the baffle pair is [by virtue of Eqs. (3.3) and (3.4) for scattering off the mirror]

$$\left(\frac{dE}{dAdt}\right)_{in} = \frac{\alpha I}{\theta^2 l_n^2} = \frac{\alpha I}{4R^2} ; \tag{4.47}$$

and correspondingly, the total power emerging from the baffle pair n, $n+1$ is [cf. the integral of (3.9) over θ']

$$\left[\frac{dE}{dt}\right]_{\text{diff.}n} = \frac{\alpha I}{4R^2}\frac{d\sigma}{dx}\pi R = \frac{\alpha I}{16\pi\theta}\frac{\lambda}{R}\frac{H}{\delta H} . \tag{4.48}$$

(Here we have approximated the total length of baffle that contributes by πR, the length of the portion on the opposite side of the pipe from the mirror.) We shall approximate the angle θ' at which this power comes off by θ. Then, since the number of baffle pairs dN_b that send their diffraction-reflected photons out in the range $d\theta$ is $dN_b = (R/H)d\theta/\theta$, the total power per unit θ crossing the midpoint of the pipe ($l = L/2$) is

$$\left[\frac{dE}{dtd\theta}\right] = \frac{\alpha I}{16\pi\theta}\frac{\lambda}{R}\frac{H}{\delta H}\frac{dN_b}{d\theta} = \frac{\alpha I}{16\pi\theta^2}\frac{\lambda}{\delta H} . \tag{4.49}$$

If there is only one set of baffles (no baffles in the second half of the pipe), then this is also the power per unit angle reaching the far end of the pipe. For comparison, the power per unit angle that started out from the scattering mirror (and that reached the far end of the pipe in the case of a LIGO without baffles) was

$$\left[\frac{dE}{dtd\theta}\right]_{\text{no baffles}} = \frac{2\pi\alpha I}{\theta} \tag{4.50}$$

[Eq. (4.42)]. Thus, the first set of baffles has succeeded in attenuating that portion of the scattered light with photon angles near θ by the factor

$$\frac{(dE/dtd\theta)_{\text{one set of baffles}}}{(dE/dtd\theta)_{\text{no baffles}}} = \frac{1}{32\pi^2}\frac{\lambda}{\delta H}\frac{1}{\theta} \approx \frac{10^{-7}}{\theta} , \tag{4.51}$$

which will range from $\sim 10^{-3}$ for the smallest relevant angles to $\sim 10^{-6}$ for the largest. The contribution of these photons to the gravitational-wave noise $\tilde{h}$ will be reduced by the square root of this number.

If there is a second set of baffles in the second half of the pipe, an analysis similar to the above will give a second reduction by the same amount as the first, so the total reduction will be the square of (4.51):

$$\frac{(dE/dtd\theta)_{\text{two sets of baffles}}}{(dE/dtd\theta)_{\text{no baffles}}} = \left[\frac{1}{32\pi^2}\frac{\lambda}{\delta H}\frac{1}{\theta}\right]^2 \approx \left[\frac{10^{-7}}{\theta}\right]^2 , \tag{4.52}$$

By inserting the reduction factor (4.51) or (4.52) into (4.42) and then repeating the calculation of Sec. III.B, one obtains the final formulas (3.25) and (3.27) for the noise $\tilde{h}(f)$. To obtain the corresponding formulas (3.26) and (3.28) for the influence of static pipe deformations μ_n on the noise, one can repeat the calculation replacing expression (4.43) for the reflection-induced modulation by

$$\tilde{\Phi}^2 = \sum_{j=1}^{N_\omega}\left[4\pi\frac{L}{\lambda}\sqrt{L\theta/2R}\,\sigma_{\mu_n}\tilde{\mu}\right]^2 = \left[\frac{4\pi L\,\sigma_{\mu_n}}{\lambda}\frac{L\theta}{2R}\tilde{\mu}\right]^2 \tag{4.53}$$

[cf. Eq. (3.8)].

D. LIGO With Baffles: Scattering of Light off the Baffles

Turn, next, to a derivation of expressions (3.29) and (3.30) for noise due to the process shown in Fig. 3.6: main-beam light scatters off a mirror toward a baffle, then scatters off the face of the baffle directly back to the mirror where it recombines with the main beam.

The foundation for the derivation is the standard noise equation (3.7), rewritten as a sum over baffles and an integral over the circumference of a baffle:

$$\tilde{h}(f) = \frac{\lambda}{2\pi BL}\left[\sum_n \int_0^{2\pi} \frac{dE_{sc}/dtdAd\phi_n df}{I/\lambda L} d\phi_n\right]^{1/2} . \tag{4.54}$$

Here $dE_{sc}/dtdA\,d\phi_n\,df$ describes the scattered light when it returns to the mirror from location ϕ_n on baffle n. We can compute this quantity as follows:

At ϕ_n on baffle n the incoming light is described by

$$\left(\frac{dE_{sc}}{dtdA}\right)_{in} = \frac{\alpha I}{l_n^2\theta^2}\,, \tag{4.55}$$

where θ is the angle at which the light must leave the mirror in order to reach location ϕ_n on baffle n. More specifically, if Y_o is the (transverse) distance of the main beam from the nearest point on the baffle and ϕ_n is measured from that nearest point, then

$$\theta = \frac{Y}{l_n}\,, \quad \text{where } Y = \sqrt{Y_o^2+2R(1-\cos\phi_n)(R-Y_o)} \tag{4.56}$$

is the transverse distance from the mirror center (or main-beam-axis) to location ϕ_n on the edge of baffle n. The light scattered back toward the mirror from a range $\Delta\phi_n$ of angles on baffle n is described by

$$\left(\frac{dE_{sc}}{dtd\Omega df}\right)_{back,\,n} = \frac{\alpha I}{l_n^2\theta^2}\left(\frac{d\sigma}{dAd\Omega}\right) RH\,\Delta\phi_n\,. \tag{4.57}$$

Here $d\sigma/dAd\Omega$ is the baffle's scattering cross section and $RH\,\Delta\phi_n$ is the cross sectional area presented by the baffle to the incoming scattered light. The energy flux of modulated light that arrives back from the baffle at the mirror is $1/l_n^2$ times (4.57), multiplied by the spectral density of the phase modulation produced by longitudinal baffle vibrations, $(4\pi\xi/\lambda)^2$ [Eq. (3.20)]:

$$\frac{dE_{sc}}{dtdA\,d\phi_n\,df} = \frac{\alpha I}{l_n^2\theta^2}\left(\frac{d\sigma}{dAd\Omega}\right)\frac{RH}{l_n^2}\left(4\pi\frac{\xi}{\lambda}\right)^2\,. \tag{4.58}$$

By inserting this (4.58) and expression (3.5) or (3.6) for $P_{rec}(\theta)$ into Eq. (4.54) and then using expression (4.56) for θ in terms of $Y(n,\phi_n)$, one obtains $\bar{h}(f)$ in a form explicitly ready for integration over ϕ_n and summation over n. The integrand turns out to be proportional to $1/Y^3$ or $1/Y^4$; and, correspondingly, the noise is stronger the closer the mirrors are to the pipe wall. We shall specialize to the case of strongest noise, Y_o as much less than R as possible. Then the integrand has a sharp peak of width $\Delta\phi_n = 2Y_o/R$ at $\phi_n = 0$, and the integral can be approximated by the value of the integrand at this peak times the peak's width. The sum over baffles can then be carried out using Eqs. (3.24) for the distances of the baffles from the mirrors, and taking account of shadowing of the baffles by each other in the first series [$n = 1$ up to $n = R/(H-\delta H)$]. This leads to the final result, Eqs. (3.29) and (3.30) for $\bar{h}(f)$.

E. LIGO With Baffles: Effects of Coherence

Throughout this report, except in Sec. III.E, we have assumed that coherence of the scattered light has a negligible influence on the noise $\bar{h}(f)$, and correspondingly we have used intensity techniques in our analyses. The impediments to coherence are great: (i) randomness in the deformations of the mirrors, which produce scattering and recombination [Eqs. (4.5) and associated discussion]; (ii) randomness in the imperfections of the photodiode, which influence recombination [Eq. (4.10) and associated discussion]; (iii) randomness in the deformations of the vacuum pipes, which redistribute reflected light randomly over the plane of the receiving mirror [discussion following Eq. (4.39)]; (iv) the Fresnel fringe pattern, which makes the cross sections for diffraction be insensitive to phase coherence [Fig. 4.5 and associated discussion]; and (v) randomness in the distance from the face of a baffle to the mirror, which makes coherence unimportant in processes involving scattering off the baffle faces.

These randomizing effects are so strong that there seems to be little to fear from coherence in any of the processes studied above, at least in the case of mirrors that are not closer to the center of the pipe than one main-beam width, $\sqrt{\lambda L}$. However, for mirrors nearer the center than this, the Fresnel fringe pattern is nearly parallel to the pipe wall and baffle edges and thus is ineffective in reducing the effects of phase coherence, and the other randomizing effects by themselves might not provide full protection. In this section we shall study this issue in detail, first for diffraction without reflection (Sec. 1) and then for combined diffraction and reflection (Sec. 2).

1. Diffraction Without Reflection

Diffraction without reflection is depicted in Fig. 4.7: Light scatters off a mirror, diffracts off the edge of a baffle, then propagates directly to the other mirror where it recombines with the main beam — all without any reflections in the pipe wall. We shall compute the noise $\tilde{h}(f)$ for this process using phase-coherent (amplitude) techniques.

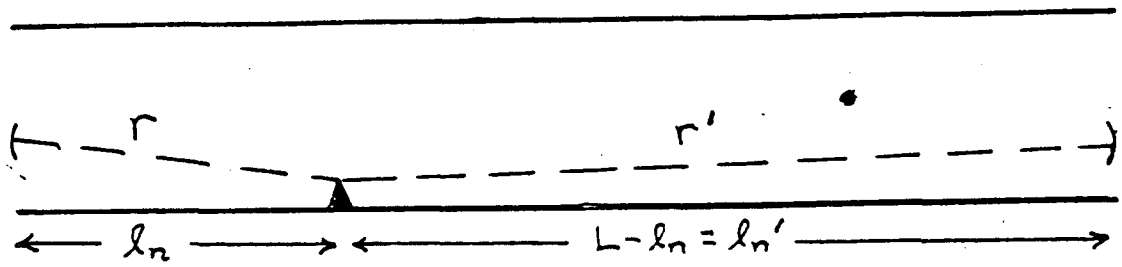

Fig. 4.7 Light scatters off a mirror, diffracts off the edge of a baffle, then propagates to the other mirror where it recombines with the main beam.

The scattering of the main beam off the scattering mirror produces the field $\psi(Y,z)$ of Eq. (4.4) at longitudinal distance z and transverse location Y from the mirror's center. This is the field that diffracts off the vibrating baffles to produce modulated light at the receiving mirror. To compute the diffracted, modulated light from baffle n at location $z = l_n$, we can insert the scattered field (4.4) into the Fresnel-Kirchoff diffraction formula [Eq. (17) of Sec. 8.3 of Born and Wolf[4]]. That diffraction formula involves an integral over the aperture bounded by the baffle. The modulation of the diffracted light is produced by vibration of the boundaries of the aperture (i.e. of the baffle); and correspondingly, the modulated diffracted field from baffle n is given by the Fresnel-Kirchoff diffraction formula restricted to the new aperture area opened up by the baffle vibrations (and with a negative contribution from old area closed off):

$$\psi_{\text{diff}\,n} = \frac{-i}{\lambda}\int_0^{2\pi} \psi \frac{e^{ikr'}}{r'}\xi_n(\phi)Rd\phi_n \ . \tag{4.59}$$

Here

$$r' = [l_n'^2 + (Y - y')^2]^{1/2} \equiv l_n' + \frac{Y^2}{2l_n'} + \frac{Y}{l_n'}\cdot y' + \frac{y'^2}{2l_n'} \tag{4.60}$$

is distance from the integration point on baffle n to location y' on the receiving mirror, with $l_n' = L - l_n$ the longitudinal distance to the receiving mirror. Also, in Eq. (4.59) $\xi_n(\phi_n)$ is the time-varying radial displacement of baffle n at location ϕ_n, $\xi_n Rd\phi_n$ is the new area opened up (negative for old area closed off) by the baffle motion, and $Y(\phi_n)$ is the transverse location of the edge of baffle n at angular location ϕ_n:

$$\mathbf{Y} = [R - \mathcal{H}(\phi_n)]\mathbf{e}_r - \frac{R - Y_o}{Y_o}\mathbf{Y}_o \ . \tag{4.61}$$

Here $\mathbf{Y}_o$ is the vector from the central axis of the main beam to the nearest point on the smoothed edge of baffle n, $\mathcal{H}(\phi_n)$ is the jaggedness-produced fluctuation in the height of baffle n (zero for a smooth baffle; a randomly fluctuating function for a jagged baffle), and $\mathbf{e}_r$ is the unit radial vector at location ϕ_n.

By inserting expressions (4.4) (with $z = l_n$) and (4.60) into (4.59) and summing over baffles, we obtain for the modulated, scattered, diffracted light arriving at location $\mathbf{y}'$ on the receiving mirror

$$\psi(\mathbf{y}') = \sum_{n=1}^{N_b} \frac{-ie^{ikL}}{\lambda l_n l_n'} e^{iky'^2/2l_n'} \int_0^{2\pi} \left[\left(\int \psi_{mb} \frac{k^2 N}{2\pi} e^{i(k\mathbf{Y}/l_n)\cdot\mathbf{y}} e^{iky^2/2l_n} d^2y \right) \right.$$

$$\left. \times e^{ikR^2/2l_{nR}} e^{i(k\mathbf{Y}/l_n')\cdot\mathbf{y}'} \xi_n R \right] d\phi_n \ , \tag{4.62}$$

where $l_{nR} \equiv l_n l_n'/L$ is the reduced length from the baffle to the mirrors. By then inserting this into Eqs (4.7) and (4.9), we obtain for h

$$h = \frac{\lambda}{2\pi BL} \text{Imaginary} \left\{ \frac{1}{I} \sum_{n=1}^{N_b} \frac{-ie^{ikL}}{l_n l_n'} \int_0^{2\pi} \left[\left(\int \psi_{mb} \frac{k^2 N}{2\pi} e^{i(k\mathbf{Y}/l_n)\cdot\mathbf{y}} e^{iky^2/2l_n} d^2y \right) \right. \right.$$

$$\left. \left. \times \left(\int \psi_{mb}(\eta/\lambda \text{ or } k^2N/2\pi) e^{i(k\mathbf{Y}/l_n')\cdot\mathbf{y}'} e^{iky'^2/l_n'} d^2y' \right) e^{ikR^2/2l_{nR}} \xi_n R \right] d\phi_n \right\} . \tag{4.63}$$

Here the expression "$(\eta/\lambda \text{ or } k^2N/2\pi)$" means to use η/λ if no mode cleaner is present so the dominant noise is due to scattered light transmitted directly to the photodiode, and otherwise use $kN^2/2\pi$ corresponding to rescattering of the light back into the main beam. In Eq. (4.63) the outer (ϕ_n) integral is over the periphery of baffle n, and the two inner integrals are over the scattering mirror ($\mathbf{y}$ integral) and the receiving mirror ($\mathbf{y}'$ integral).

We shall now treat separately detectors with and without mode cleaners on their outputs:

1a. With Mode Cleaner

When there is a mode cleaner present the two inner integrals in (4.63) are both given by Eq. (4.5c), and (4.63) is thereby brought into the form

$$h = \frac{\alpha\lambda}{2\pi BL} \text{Imaginary} \left[\sum_{n=1}^{N_b} -ie^{ikL} \int_0^{2\pi} e^{ikR^2/2l_{nR}} f_{sm}(\mathbf{Y}) f_{rm}(\mathbf{Y}) \frac{R\xi_n}{Y^2} d\phi_n \right] . \tag{4.64}$$

Here $f_{sm}(\mathbf{Y})$ is the fluctuating function that comes from the $\mathbf{y}$ integral over the scattering mirror, and $f_{rm}(\mathbf{Y})$ is the analogous function from the $\mathbf{y}'$ integral over the receiving mirror.

Specialize, now, to the case of mirrors that are far from the center of the vacuum pipe. In this case the exponential in the integrand of (4.64) is the Fresnel fringe pattern that is depicted in Fig. 4.8, superimposed on a smooth baffle. Each Fresnel zone in the pattern (each region over which the phase changes by π) has a width

$$\Delta Y = \frac{l_{nR}}{L} \frac{\lambda L}{2Y} \sim (\text{a few mm}) ; \tag{4.65}$$

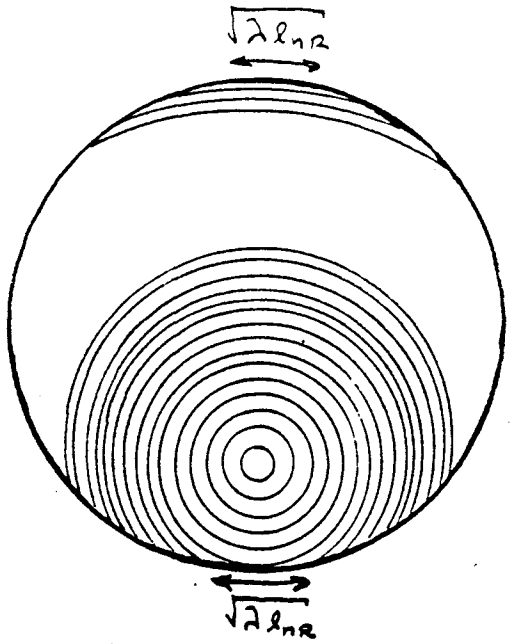

Fig. 4.8 The Fresnel pattern of the exponential term in the integral (4.64) superimposed on a smooth baffle.

see Fig. 4.8. This fringe pattern is parallel to the pipe walls at the bottom and the top of the pipe (Fig. 4.8); and if the baffle edges are circular rather than jagged [if $H = 0$ in Eq. (4.61)], then the bottom and top Fresnel zones will occupy a lateral piece of baffle edge of length $\sqrt{\lambda L}$.

By carrying out an analysis completely analogous to that of Eqs. (4.24)—(4.29) one can show that the integral (4.64) is almost completely insensitive to the fluctuations with ϕ_n of the functions $f_{sm}(Y)$, $f_{rm}(Y)$, and $H(\phi_n)$. Independently of these functions the rms value of the integral is $\sqrt{\lambda L_{nR}}\,\xi_n(\phi_n = 0, t)/Y_o^2$; and correspondingly, the square root of the spectral density of h is

$$\bar{h} = \frac{\alpha\lambda}{2\pi BL}\frac{\sqrt{\lambda L}\,\bar{\xi}}{Y_o^2}\left[\sum_n \frac{l_{nR}}{L}\right]^{1/4} . \tag{4.66}$$

By carrying out the sum with the aid of the baffle spacings (3.24) we obtain the following final formula for the noise:

$$\begin{aligned}\bar{h} &= \frac{\sqrt{3}}{4\pi}\frac{\alpha}{B}\left[\frac{\lambda}{L}\right]^{1/4}\left[\frac{\sqrt{\lambda L}}{Y_o}\right]^2\left[\frac{R}{H-\delta H}\right]^{1/4}\frac{\bar{\xi}}{L} \\ &= \frac{2\times 10^{-29}}{\sqrt{\text{Hz}}}\left[\frac{10\,\text{Hz}}{f}\right]\frac{\bar{\xi}}{10^{-7}\,\text{cm Hz}^{-1/2}\,(10\,\text{Hz}/f)^2} .\end{aligned} \tag{4.67}$$

This is the same result as one obtains by doing the calculation with the amplitude techniques of Sec. IV.A.

Thus, *in the case of mirrors far from the center of the pipe, the Fresnel pattern by itself gives full protection against phase coherence.* [Note: Because of the extremely small value of the noise (4.67), we ignore it in the summary of major noise sources in Sec. III.]

Turn, next, to the idealized case of mirrors precisely at the center of the vacuum pipe, and baffles that are perfectly round and perfectly aligned with the mirrors. Then the Fresnel fringe pattern is precisely parallel to the baffles, and correspondingly $Y^2 = (R-H)^2 - 2(R-H)H(\phi_n)$; and expression (4.64) for the noise reduces

to

$$h = \frac{\alpha\lambda}{2\pi BL}\,\text{Imaginary}\left[\sum_{n=1}^{N_b} -ie^{ikL}e^{ik(R-H)^2/2L_m}\int_0^{2\pi} e^{[ik(R-H)/L_m]H(\phi_n)} f_{sm}(\mathbf{Y}) f_{rm}(\mathbf{Y})\frac{\xi_n}{R}d\phi_n\right] . \tag{4.68}$$

The most dangerous situation would be one with (i) perfectly smooth baffles, so $H(\phi_n) = 0$, (ii) mirrors with imperfections that are perfectly circularly symmetric about the axis of the main beam, so that $f_{sm}(\mathbf{Y})$ and $f_{rm}(\mathbf{Y})$ are independent of ϕ_n along the periphery of baffle n, and (iii) acoustic vibrations of the baffles that are perfectly circularly symmetric so that $\xi_n(t)$ is independent of ϕ_n. Then the modulus of the integral would be $2\pi\xi_n/R$, and the spectral density of $\bar{h}$ would work out to be

$$\begin{aligned}\bar{h} &= \frac{\alpha}{B}\left[\frac{\lambda}{L}\right]^{1/2}\left[\frac{\sqrt{\lambda L}}{R}\right]\sqrt{N_b}\,\frac{\bar{\xi}}{L} \\ &= \frac{1\times10^{-27}}{\sqrt{\text{Hz}}}\left[\frac{10\,\text{Hz}}{f}\right]\frac{\bar{\xi}}{10^{-7}\,\text{cm Hz}^{-1/2}(10\,\text{Hz}/f)^2} ,\end{aligned} \tag{4.69}$$

where N_b, the number of baffles, is given by Eq. (2.5). This is still too small to be of concern.

In reality, the mirror irregularities will not be perfectly circularly symmetric. Rather, they are likely to give rise to functions $f_{sm}(\mathbf{Y})$ and $f_{rm}(\mathbf{Y})$ that vary on lengthscales $\sigma_M \sim \sqrt{\lambda L}$. This will reduce the modulus of the integral (4.68) and thence the noise level (4.69) by a factor $\sqrt{\sigma_M/2\pi R} \sim 0.1$:

$$\bar{h} = [\text{Expression (4.69)}]\times\left[\frac{\sigma_M}{2\pi R}\right]^{1/2} \quad \text{if } f_{sm} \text{ and } f_{rm} \text{ vary on the scale } \sigma_M . \tag{4.70a}$$

If, in addition, the baffles are made jagged in accord with Recommendation 3, on transverse scales $\sigma_H \sim 1$ mm, then the integral (4.68) and the noise (4.67) will be reduced by a factor $\sqrt{\sigma_H/2\pi R} \sim 0.01$:

$$\bar{h} = [\text{Expression (4.69)}]\times\left[\frac{\sigma_H}{2\pi R}\right]^{1/2} \quad \text{if baffles are jagged on scale } \sigma_H . \tag{4.70b}$$

Such jaggedness is not needed to control the noise (4.69) in this case of a mode cleaner on the output; but when there is no mode cleaner, the noise is larger and jaggedness might be desirable:

1b. Without Mode Cleaner

In the absence of a mode cleaner recombination occurs directly in the photodiode. In this case a calculation patterned directly after the above gives the following results:

When the mirrors are far from the center of the pipe, the Fresnel pattern protects completely against coherent effects, and the noise has the same form as would be predicted by an intensity analysis:

$$\begin{aligned}\bar{h} &= \frac{\sqrt{6}}{4\pi}\,\frac{\sqrt{\alpha}(1-\bar{\eta})}{B}\left[\frac{\lambda}{L}\right]^{1/2}\left[\frac{\sqrt{\lambda L}}{Y_o}\right]^{3/2}\left[\frac{R}{H-\delta H}\right]^{1/2}\frac{\bar{\xi}}{L} \\ &= \frac{7\times10^{-27}}{\sqrt{\text{Hz}}}\left[\frac{10\,\text{Hz}}{f}\right]\frac{\bar{\xi}}{10^{-7}\,\text{cm Hz}^{-1/2}(10\,\text{Hz}/f)^2} .\end{aligned} \tag{4.71}$$

This is too small to be of concern, so it is not discussed among the serious noise sources in Sec. III.

When the mirrors are at the center of the vacuum pipe and have perfectly circular irregularities centered on the main-beam axis, and the baffles are perfectly smooth, and the baffles vibrate perfectly circularly, then coherence is very important and the noise level works out to be

$$\tilde{h} = \frac{\sqrt{\bar{\alpha}(1-\bar{\eta})}}{B}\left[\frac{\lambda}{L}\right]^{1/2}\left[\frac{\sqrt{\lambda L}}{R}\right]^{1/2}\left[\frac{R}{H-\delta H}\right]^{1/2}\left[\frac{L\theta_{\rm rms}}{R}\right]^{1/2}\frac{\xi}{L}$$

$$= \frac{3\times10^{-24}}{\sqrt{\rm Hz}}\left[\frac{10\,{\rm Hz}}{f}\right]\frac{\xi}{10^{-7}\,{\rm cm\,Hz^{-1/2}}(10\,{\rm Hz}/f)^2} . \qquad (4.72)$$

This is the same noise level as the standard quantum limit. Noncircular irregularities in the mirror and photodiode will reduce this noise by the same factor (4.70a) as in the case with a mode cleaner, perhaps bringing the noise down by one order of magnitude. Jaggedness of the baffles would bring the noise down by the factor (4.70b), perhaps two orders of magnitude.

Equations (4.69), (4.70), and (4.72) for the case of mirrors at the pipe center are reproduced and discussed further in Sec. III.E.1 [Eqs. (3.31)].

2. Diffraction with Reflection

The above analysis was for the simplest process in which coherence might be important: Diffraction with no accompanying reflections. We now turn to the effects of coherence in the more complicated and more noisy situation of diffraction plus reflections. It seems rather clear (though I have not proved it rigorously) that for mirrors far from the pipe center the Fresnel pattern will protect fully against coherence; see the paragraph following Eq. (4.29). Therefore we shall consider only mirrors at the pipe center. We shall begin by restricting attention to a LIGO with just one set of baffles (Sec. 2a); and we then shall extend the analysis to the case of two sets of baffles (Sec. 2b).

2a. One Set of Baffles

We presume, in this subsection, that the inner half of the vacuum pipe (the half nearest the corner mirror) is baffled in the manner of Eqs. (3.24), but the outer half has no baffles. For such a LIGO we shall compute, using phase-coherent techniques, the noise due to the combined effects of diffraction-aided reflection and ordinary reflection (Fig. 3.5), together with ordinary diffraction and ordinary reflection (Fig. 3.1).

Throughout our analysis we shall assume that the mirrors are precisely at the center of the vacuum pipe (the most dangerous situation). The pipe will be presumed slightly crooked, so that relative to the central axis of the main beam the pipe's central axis is displaced by an amount $\vec{\xi}_o(l)$. Here l is distance down the pipe from the corner mirror. This means that the distance from the main-beam axis to the wall, at longitudinal location l and azimuthal location ϕ, is $R+\varpi(\phi,l)$, where

$$\varpi(\phi,l) = \xi_o(l)\cos[\phi-\phi_{\xi_o}(l)] . \qquad (4.73)$$

Here $\xi_o(l)$ is the magnitude of $\vec{\xi}_o(l)$ and $\phi_{\xi_o}(l)$ is its direction. For simplicity we shall assume that the pipe is perfectly round, though it would not be difficult to generalize to the case of a deformed pipe. To do so one should add onto expression (4.73) a quadrupolar term $\xi_2\cos[2\phi-2\phi_2(l)]$ and terms of higher order. We shall presume that ξ_o and ϕ_{ξ_o} vary randomly on lengthscales shorter than or of order the separations between baffles; we shall denote by σ_ξ the rms value of ξ_o; and for numerical estimates we shall use $\sigma_\xi = 1$ cm. As we shall see, this crookedness of the pipe impedes the focusing of scattered light and impedes phase-coherent effects. Random variations in the pipe's roundness could also serve this purpose.

In our analysis we shall break into components the scattered light arriving at the receiving mirror. Each component reflects off the walls a specific number of times N and then terminates its reflection by diffracting off baffle n, or by a diffraction-aided reflection at baffle pair n, $n+1$ (Fig. 3.5a viewed with propagation from right to left). Thus, each component will be characterized by the two integers (n,N) and by a statement as to whether it terminates with a pure diffraction ("diff") or with a diffraction-aided reflection ("DAR"). The

randomness of the pipe crookedness and randomness in the acoustic noise on the pipe should make random the relative phases of the light's various components; but phase coherence could be important for each individual component.

As in previous sections we shall denote by

$$\theta_n = 2H/s_n \simeq 2R/l_n \tag{4.74a}$$

the critical angle for baffle n. Any light with $\theta < \theta_n$ will be unable to make wall reflections nearer the corner mirror than baffle n. The components (n,N,diff) and (n,N,DAR) will have, before they reach baffle n, an angle $\theta \equiv \theta_{nN}$ given by

$$\theta_{nN} = \frac{R(2N-1)}{l'_n} \simeq N\frac{2R}{l'_n}, \quad \text{where } l'_n \equiv L - l_n . \tag{4.74b}$$

In order to reach the receiving mirror, these components must diffract to the angle

$$\theta'_n = \frac{R-H}{l_n} \simeq \frac{R}{l_n} . \tag{4.74c}$$

Note that because $s_n/l_n = R/H$ [Eqs. (3.24)],

$$\theta'_n \simeq \frac{\theta_n}{2} . \tag{4.75}$$

This should be contrasted with $\theta'_n = (1-\delta H/H)\theta_n$ in the case of mirrors near the pipe's walls. In effect, the centered mirrors are protected by a height-safety factor of $\delta H_{\text{eff}} = H/2$. This added protection, compared to $\delta H = H/6$ for near-wall mirrors, suppresses the cross section for diffraction-aided-reflection, making it approximately equal to that for ordinary diffraction — and thereby forces us to consider both types of diffraction in our analysis.

The number of reflections N for a given component of the scattered light is limited by the requirement that the light reach baffle n without being stopped by any previous baffles, and then undergo either an ordinary diffraction or a diffraction-aided reflection. These requirements turn out to restrict N to the range

$$1 \le N \le \frac{\theta_o L}{2R} \quad \text{for ordinary diffraction} , \tag{4.76a}$$

$$\frac{l'_n}{l_n} \le N \le \frac{\theta_o L}{2R} \quad \text{for diffraction-aided reflection} . \tag{4.76b}$$

The modulation put onto the light by acoustic vibrations of the walls at the reflection points is much greater than the modulation put on by vibrations of the diffracting baffles. Consequently, the modulational fluctuations in phase shift of the (n,N) components, when they arrive at the receiving mirror, will be

$$\delta\Phi_{nN} = \sum_{j=1}^{N} 4\pi \left[\frac{(L-2l_j)\theta_{nN} + L\sqrt{L\theta_{Nn}/2R}\ \sigma_{\mu L}}{\lambda} \right] \delta\mu(\phi, l_j, t) \tag{4.77}$$

[cf. Eq. (4.17b)]. Here j labels the various reflections, l_j is the longitudinal location of reflection j, t is time, and ϕ is the angular location of a specific set of photons in component (n,N). (Because the light's transverse motion is nearly radial, each photon has nearly constant ϕ, except for jumps of π when going through the pipe's central axis.)

With these preliminaries taken care of, we are now ready to evaluate the contribution of the components (n,N) to the scattering noise. The field scattered off the end mirror into angle θ_{nN} is described, before it

reaches its first reflection point, by

$$\psi = \left(\frac{\alpha I}{\theta_{nN}^2} \right)^{1/2} \frac{1}{r} e^{ikr} f_{sm} , \tag{4.78}$$

where f_{sm} is the slowly varying function discussed in Eqs. (4.5). The subsequent propagation up to baffle n can be described by geometric optics [phase change equal to k times distance traveled by rays; amplitude proportional to 1/(radius of curvature of wave fronts); and wall-induced modulation given by Eq. (4.77)]. Upon arriving at the vicinity of baffle n, the wave fronts have radii of curvature l'_n in the radial direction and R/θ_{nN} = (transverse distance back to last focal point) in the azimuthal direction; so their net radius of curvature (geometric mean of these two) is $\sqrt{l'_n R/\theta_{nN}}$. Correspondingly, the modulated part of the field in the vicinity of baffle n is

$$\psi_{in} = i\,\delta\Phi_{nN} \left(\frac{\alpha I}{\theta_{nN} l'_n R} \right)^{1/2} e^{i\Phi_{nN}} f_{sm} . \tag{4.79}$$

Here Φ_{nN} is ik times the total distance travelled by the rays since leaving the center of the scattering mirror:

$$\Phi_{nN} = k \left[l'^2_n + [R - H - \rho + \sum_{j=1}^{N} (2R + 2\varpi_j)]^2 \right]^{1/2}$$

$$= \text{const} + 2k\theta_{nN} \sum_{j=1}^{N} \varpi_j - k\theta_{nN}\rho + \frac{k}{2} \frac{l'_n}{R^2} \theta_{nN}^2 \rho^2 , \tag{4.79}$$

where $\varpi_j = \varpi(\phi + j\pi, l_j)$ is the lateral offset of the pipe at reflection point j as given by Eq. (4.73), and ρ is height above the level of the smoothed baffle (the mean level about which baffle jaggedness oscillates). The quantity $\sum_{j=1}^{N} \varpi_j$, being a sum of circular harmonics of order 1, is itself a circular harmonic of order 1 and has the value

$$\sum_{j=1}^{N} \varpi_j = \sqrt{N}\, \sigma_\xi \cos(\phi - \bar{\phi}_\xi) ,$$

where σ_ξ is the rms pipe offset and $\bar{\phi}_\xi$ is a mean phase of offset, which will vary randomly from one light component (n,N) to another. Correspondingly, the phase of the light in the plane above baffle n (aside from the slowly varying factor f_{sm}) is the following function of height ρ and azimuthal angle ϕ

$$\Phi_{nN} = \text{const} + 2k\theta_{nN}\sqrt{N}\, \sigma_\xi \cos(\phi - \bar{\phi}_\xi) + k\theta_{nN}\rho + \frac{k}{2} \frac{l'_n}{R^2} \theta_{nN}^2 \rho^2 . \tag{4.80}$$

To recapitulate, (4.79) is the modulated field coming into the plane of baffle n after N reflections; and in this expression the rapidly varying phase factor is (4.80), and the modulation factor is (4.77).

We note in passing that expression (4.79), with the modulation $i\,\delta\Phi_{nN}$ stripped off, gives for the total energy flux in the vicinity of the centermost baffle (where N runs from 1 to $\theta_n L/2R$ for both the diff and DAR components; i.e. where the DAR components have not yet been subjected to any attenuation)

$$|\psi_{tot}|^2 = 2 \sum_{N=1}^{\theta_n L/2R} \frac{\alpha I}{\theta_{nN} l'_n R} = 2 \sum_{N=1}^{\theta_n L/2R} \frac{\alpha I}{2NR^2} = \frac{\alpha I}{R^2} \ln\left(\frac{\theta_n L}{2R} \right) . \tag{4.81}$$

Here the factor 2 takes account of the two, diff and DAR, types of components (i.e. of light that most recently was reflected from the far wall, and of that most recently reflected from the near wall). Note that this energy flux at the baffle edge is 1/2 the average energy flux in the baffle plane, i.e. 1/2 of

$$\frac{1}{\pi R^2}\int_{2R/L}^{\theta_c}\frac{\alpha I}{\theta^2}2\pi\theta d\theta=\frac{2\alpha I}{R^2}\ln\left(\frac{\theta_c L}{2R}\right).$$

The factor of 1/2 presumably is because of the focusing of the light toward the center of the pipe by reflection off the walls. The agreement to within a factor 1/2 indicates that we have correctly deduced the amplitude of the incoming light ψ_{in} in (4.77).

We now shall study, for several paragraphs, ordinary diffraction of the incoming light (4.77) by baffle n; i.e. we shall set aside, momentarily, the DAR component and deal only with the diff component. The incoming light, by diffracting off the baffle, produces the following field at transverse location $\mathbf{y}'$ on the receiving mirror

$$\psi(\mathbf{y}')=\frac{i}{\lambda l_n}\int_0^{2\pi R-H}\int_{H(\phi)}\psi_{in}(\rho,\phi)e^{ikl_n}e^{ik(\mathbf{Y}+\mathbf{y}')^2/2l_n}Rd\rho d\phi\,. \tag{4.82}$$

Here $\mathbf{Y}$ is the vector describing the transverse location of the point (ρ,ϕ) in the plane of the baffle, relative to the main-beam axis; and expression (4.82) is an explicit version of the Fresnel-Kirchoff diffraction formula.

By inserting the field (4.82) into the phase-coherent expressions (4.7) and (4.9) for the gravitational-wave noise $h(t)$ and using Eqs. (4.5c) and (4.10) to evaluate the integrals over the receiving mirror, we obtain the following phase-coherent expressions for the noise due to component (n,N,diff):

$$h_{nN\,\text{diff}}(t)=\frac{\sqrt{\alpha}}{2\pi BL}\left(\frac{\lambda L}{I}\right)^{1/2}\left(\frac{\lambda}{L}\right)^{1/2}\text{Imaginary}\left[\frac{ie^{ikl_n}}{\lambda}\int_0^{2\pi}\int_{H(\phi)}^{R}\psi_{in}e^{ik\mathbf{Y}^2}f_{rm}(\mathbf{Y})d\rho d\phi\right]\quad\text{with mode cleaner,}\tag{4.83a}$$

$$h_{nN\,\text{diff}}(t)=\frac{(1-\bar{\eta})}{2\pi BL}\left(\frac{\lambda L}{I}\right)^{1/2}\left(\frac{\lambda}{L}\right)^{1/4}\left(\frac{R}{l_n}\right)^{1/2}\text{Imaginary}\left[\frac{ie^{ikl_n}}{\lambda}\int_0^{2\pi}\int_{H(\phi)}^{R}\psi_{in}e^{ik\mathbf{Y}^2}f_{pd}(\mathbf{Y})d\rho d\phi\right]$$

$$\text{without mode cleaner,}\tag{4.83b}$$

By inserting into (4.83) expressions (4.79), (4.77), and (4.80) for ψ_{in} and then evaluating the spectral density of the resulting $h_{nN\,\text{diff}}$, we obtain

$$\tilde{h}_{nN\,\text{diff}}(f)=\frac{\sqrt{2}}{3}\frac{\alpha}{B}\left(\frac{\lambda}{L}\right)^{1/2}\frac{\sqrt{\lambda L}}{R}A_{nN}^{\text{diff}}\tilde{\mu}\quad\text{with mode cleaner,}\tag{4.84a}$$

$$\tilde{h}_{nN\,\text{diff}}(f)=\frac{1}{3}\frac{\sqrt{\alpha}(1-\bar{\eta})}{B}\left(\frac{\lambda}{L}\right)^{1/2}\left(\frac{\sqrt{\lambda L}}{R}\right)^{1/2}\left(\frac{L}{l_n}\right)^{1/2}A_{nN}^{\text{diff}}\tilde{\mu}\quad\text{without mode cleaner.}\tag{4.84b}$$

where

$$A_{nN}^{\text{diff}}=(\theta_{nN}+3\sqrt{L\theta_{nN}/2R}\;\sigma_{\mu})I_{\rho\phi}\tilde{\mu}\,.\tag{4.84c}$$

Here the integral over the baffle plane has been embodied in the quantity

$$I_{\rho\phi}=\left|\frac{1}{\lambda}\int_0^{2\pi}d\phi\exp[i2k\sqrt{N}\;\theta_{nN}\sigma_{\xi}\cos(\phi-\bar{\phi}_{\xi})]f_{sm}f_{rm\text{ or }pd}f_{\mu}\int_{H(\phi)}^{\infty}\exp\left[ik\left(-(\theta_{nN}+\theta'_n)\rho+\frac{1}{2}\frac{\rho^2}{l_n}+2N^2\frac{\rho^2}{l'_n}\right)\right]d\rho\right|.\tag{4.84d}$$

Here $f_{\mu}(\phi)$ is a slowly varying function of ϕ which, like the other f functions, has rms value unity, and which

characterizes the angular dependence of the acoustic noise μ. The integral over ρ is a Fresnel integral with argument in the regime (4.33c). By performing that integral we obtain

$$I_{\rho\phi} = \frac{1}{(\theta_{nN}+\theta'_n)} \left| \frac{1}{2\pi} \int_0^{2\pi} d\phi \exp[i 2k\sqrt{N}\,\theta_{nN}\sigma_{\xi_\perp}\cos(\phi-\bar{\phi}_{\xi_\perp})] G(\phi) d\phi \right| , \tag{4.85a}$$

where

$$G(\phi) = e^{ik(\theta_{nN}+\theta'_n)\mathcal{H}(\phi)} f_{sm}(\phi) f_{rm\ or\ pd}(\phi) f_{\mu}(\phi) \tag{4.85b}$$

is a function with rms value unity that incorporates all azimuthal variations due to baffle jaggedness ($\mathcal{H}$), irregularities of the scattering mirror (f_{sm}), irregularities of the receiving mirror or photodiode ($f_{rm\ or\ pd}$), and angular variations of the pipe's acoustic noise (f_{μ}).

Phase-coherent effects would be the most serious if G were independent of ϕ (smooth baffles, perfectly circular irregularities of mirrors and photodiode, perfectly radial acoustic vibrations). In this case the phase factor $i 2k\sqrt{N}\,\theta_{nN}\sigma_{\xi_\perp}\cos(\phi-\bar{\phi}_{\xi_\perp})$, which describes a Fresnel fringe pattern that is offset from the baffle edge by a distance $\sqrt{N}\,\theta_{nN}\sigma_{\xi_\perp}$, would force almost all the net contribution to $I_{\rho\phi}$ to come from two opposite regions on the baffle edge, regions with length

$$\Delta x \equiv R\Delta\phi = \left[\frac{\lambda l'_n}{N} \frac{R}{4N^{1/2}\sigma_{\xi_\perp}} \right]^{1/2} . \tag{4.86}$$

As we shall see below, the noise $\tilde{h}(f)$ is dominated by light whose number of reflections is $N \sim l'_n/l_n$. This means that, if the pipe is so crooked that $\sigma_{\xi_\perp} \geq 1$ cm, then Δx will be so small

$$\frac{\Delta x}{(l_n/L)\sqrt{\lambda L}} = \left[\frac{R}{4\sigma_{\xi_\perp}} \right]^{1/2} \left[\frac{L^2}{l_n l'_n} \right]^{1/4} \lesssim 4 \tag{4.87}$$

that the baffle can feed light to only a few modes of the mirror [cf. discussion following Eq. (4.11)]. This, in turn, means that effects of phase coherence cannot be great. The random fluctuations of baffle jaggedness, noncircular mirror and photodiode irregularities, and acoustic-noise angular variations (which are embodied in a non-unit value of G) can only make phase coherence even less important. Despite this unimportance of phase coherence, we shall continue our phase-coherent analysis:

For arbitrarily varying G we can evaluate the integral (4.85a) by Fourier transform techniques: First we characterize $G(\phi)$ and the exponential factor in (4.85) by their Fourier coefficients:

$$G(\phi) = \sum_{m=-\infty}^{+\infty} g_m e^{im\phi} , \tag{4.88a}$$

$$\exp[i 2k\sqrt{N}\,\theta_{nN}\sigma_{\xi_\perp}\cos(\phi-\bar{\phi}_{\xi_\perp})] = \sum_{m=-\infty}^{+\infty} J_{|m|}(2k\sqrt{N}\,\theta_{nN}\sigma_{\xi_\perp}) e^{im(\phi-\bar{\phi}_\xi)} . \tag{4.88b}$$

Here $J_{|m|}$ is the ordinary bessel function of order $|m|$. The Fourier coefficients g_m, henceforth will be surrogates for $G(\phi)$. By inserting the expansions (4.88) into (4.85a) and integrating, we obtain

$$I_{\rho\phi} = \frac{1}{(\theta_{nN}+\theta'_n)} \left| \sum_{m=-\infty}^{+\infty} g_m J_{|m|}(2k\sqrt{N}\,\theta_{nN}\sigma_{\xi_\perp}) \right| .$$

Because the function $G(\phi)$ is more or less random, the relative phases of the g_m's will be random with respect to each other. This means that the square root of the square of the above expression will be

$$I_{\rho\phi} = \frac{1}{(\theta_{nN}+\theta'_n)} \left[\sum_{m=0}^{+\infty} (|g_m|^2+|g_{-m}|^2) J_m^{\,2}(2k\sqrt{N}\,\theta_{nN}\sigma_{\xi_\perp}) \right]^{1/2} . \tag{4.89}$$

The quantity $(|g_m|^2 + |g_{-m}|^2)$ is the precise analog, in this periodicity-of-ϕ situation, of the spectral density of $G(\phi)$. One should, in fact, think of it as G's spectral density; and one should think of the $J_m^2(2k\sqrt{N}\,\theta_{nN}\sigma_{\xi_\perp})$ in (4.89) as the square of a filter function (with m the argument of the filter function, i.e. the "frequency" at which it is evaluated). The input to the filter is $G(\phi)$; its output is the $I_{\rho\phi}$ of Eq. (4.85a); and the rms value of this output is expression (4.89).

Note that the parameter u appearing in the filter function $J_m(u)$ has magnitude

$$u = 8\pi N^{3/2}\frac{R}{l'_n}\frac{\sigma_{\xi_\perp}}{\lambda} \geq 100\,. \tag{4.90}$$

In this regime it is a reasonable approximation to set

$$J_m^2(u) \simeq \frac{1}{\pi u} \quad \text{for } m < u\,,$$
$$J_m^2(u) = 0 \quad \text{for } m > u\,, \tag{4.91}$$

and correspondingly to write (4.89) in the form

$$I_{\rho\phi} \simeq \frac{1}{\sqrt{8\pi^2 N^{3/4}(\theta_{nN}+\theta'_n)}}\left(\frac{\lambda l'_n}{R\,\sigma_{\xi_\perp}}\right)^{1/2} S\,. \tag{4.92}$$

Here

$$S \equiv \sum_{m=0}^{8\pi N^{3/2} R\,\sigma_{\xi_\perp}/(l'_n\lambda)} (|g_m|^2 + |g_{-m}|^2) \tag{4.93a}$$

is the rms value of $G(\phi)$ after filtering it to remove all Fourier components with $m > u \equiv 8\pi N^{3/2} R\,\sigma_{\xi_\perp}/(l'_n\lambda)$. Thus, only $G(\phi)$'s Fourier components of low order $|m| < u$ are able to diffract light. The high-order components do not diffract.

Because f_{sm}, f_{rm}, f_{pd}, and f_μ are not likely to contain any substantial Fourier components of order $|m| \geq 100$ (the minimum value of u), they will have no significant influence on the $I_{\rho\phi}$ of Eq. (4.89). More specifically, in the absence of baffle jaggedness, the "suppression factor" S will be unity (no suppression) independently of the fluctuations due to angular irregularities of the scattering mirror, receiving mirror, photodiode, and acoustic noise. This is a precise analog, for centered mirrors but crooked pipes, of the insensitivity of diffracted light to angular irregularities in the case of mirrors near the walls [Eq. (4.29) and preceding discussion]. Thus, we henceforth can ignore the angular irregularites of the mirrors, photodiode, and acoustic noise, and can focus attention solely on those due to baffle jaggedness.

In order to suppress the scattered light substantially, we must take care that the baffles' jaggedness does not contain substantial Fourier components with $|m| < u$. This is the origin of the statement in Recommendation 3 (Sec. II.3) that the baffles should "have the shortest wavelength σ_H that can be achieved without great effort, preferably $\ll 1$ cm"; and that they should "contain as little longer wavelength component as can be achieved without undue effort". Henceforth we shall assume that this recommendation has been implemented. Then we can regard the suppression factor S as a function of $\sigma_H/2\pi Ru$:

$$S = S(\sigma_H/2\pi Ru) = S\left(\frac{4N^{3/2}\sigma_{\xi_\perp}\sigma_H}{l'_n\lambda}\right)\,. \tag{4.93b}$$

and this function [defined rigorously by Eqs. (4.89) and (4.92), and approximated by (4.93a)] will have the properties described in Eq. (3.34) of Sec. III.E. Note that in order to achieve significant noise suppression, the maximum wavelength of baffle jaggedness must be much shorter than

$$\sigma_{H\,\min} = \frac{l'_n \lambda}{4N^{3/2}\sigma_{\xi_\mu}} < \frac{L\lambda}{8\sigma_{\xi_\mu}} = 2\,\text{cm}\left[\frac{1\,\text{cm}}{\sigma_{\xi_\mu}}\right] . \tag{4.94}$$

This is the reason that the jaggedness wavelength is specified in Recommendation 3 to be "preferably $\ll 1$ cm".

Let us return to our calculation of the scattering noise. By combining Eqs. (4.84c) and (4.92) we obtain

$$A_{nN}^{\text{diff}} = \left[\frac{1}{8\pi^2}\frac{\lambda l'_n}{R\sigma_{\xi_\mu}}\right]^{1/2} \frac{1}{N^{3/4}} \frac{(\theta_{nN}+3\sqrt{L\theta_{nN}/2R}\;\sigma_{\mu_\mu})}{(\theta_{nN}+\theta'_n)} S\left[\frac{4N^{3/2}\sigma_{\xi_\mu}\sigma_H}{l'_n\lambda}\right] \quad \text{for } 1 \le N \le \frac{\theta_o L}{2R} . \tag{4.95a}$$

This is the factor for ordinary diffraction which appears in expressions (4.84) for the noise. It should be fairly obvious that the same calculation for diffraction-aided reflection will lead to the same expression, but with $\theta_{nN}+\theta'_n$ in the denominator replaced by $\theta_{nN}-\theta'_n$:

$$A_{nN}^{\text{DAR}} = \left[\frac{1}{8\pi^2}\frac{\lambda l'_n}{R\sigma_{\xi_\mu}}\right]^{1/2} \frac{1}{N^{3/4}} \frac{(\theta_{nN}+3\sqrt{L\theta_{nN}/2R}\;\sigma_{\mu_\mu})}{(\theta_{nN}-\theta'_n)} S\left[\frac{4N^{3/2}\sigma_{\xi_\mu}\sigma_H}{l'_n\lambda}\right] \quad \text{for } \frac{l'_n}{l_n} \le N \le \frac{\theta_o L}{2R} . \tag{4.95b}$$

Since different components (n,N,diff) and (n,N,DAR) will have random relative phases and thus contribute incoherently to the noise relative to each other, the total noise will have the form [cf. Eqs. (4.84) and (4.95)]

$$\tilde{h} = \frac{\sqrt{2}}{3}\frac{\alpha}{B}\left[\frac{\lambda}{L}\right]^{1/2}\frac{\sqrt{\lambda L}}{R}\tilde{\mu}\left[\sum_{n=1}^{N_h}\left[\sum_{N=1}^{\theta_o L/2R}(A_{nN}^{\text{diff}})^2 + \sum_{N=l'_n/l_n}^{\theta_o L/2R}(A_{nN}^{\text{DAR}})^2\right]\right]^{1/2} \quad \text{with a mode cleaner,} \tag{4.96a}$$

$$\tilde{h} = \frac{1}{3}\frac{\sqrt{\alpha}(1-\bar{\eta})}{B}\left[\frac{\lambda}{L}\right]^{1/2}\left[\frac{\sqrt{\lambda L}}{R}\right]^{1/2}\tilde{\mu}\left[\sum_{n=1}^{N_h}\frac{L}{l_n}\left[\sum_{N=1}^{\theta_o L/2R}(A_{nN}^{\text{diff}})^2 + \sum_{N=l'_n/l_n}^{\theta_o L/2R}(A_{nN}^{\text{DAR}})^2\right]\right]^{1/2} \quad \text{without a mode cleaner.} \tag{4.96b}$$

Examination of expressions (4.95a,b) shows that: (i) the diff and DAR components contribute approximately equally to the sum over N = (number of reflections); and (ii) the sum is dominated, for both diff and DAR, by reflections numbers $N \sim l'_n/l_n$ — i.e. by light for which the incoming angle θ_{nN} is approximately twice the diffracted angle θ'_n [cf. Eqs. (4.74)]. (This is in accord with assumptions made in this report's intensity analyses.) The actual result of summing over N is

$$\sum_{N=1}^{\theta_o L/2R}(A_{nN}^{\text{diff}})^2 + \sum_{N=l'_n/l_n}^{\theta_o L/2R}(A_{nN}^{\text{DAR}})^2 = \frac{11}{16\pi^2}\frac{\lambda\sqrt{l_n l'_n}}{R\sigma_{\xi_\mu}}\left[1+3\frac{Ll_n}{R^2}\sigma_{\mu_\mu}{}^2\right]\left[S\left[\frac{4(l'_n/l_n)^{3/2}\sigma_{\xi_\mu}\sigma_H}{\lambda l'_n}\right]\right]^2 . \tag{4.97}$$

Here we have approximated the net effect of the suppression factor S by the function $S(x)$ evaluated for $N = l'_n/l_n$.

The final step in our derivation of the noise $\tilde{h}$ for a single set of baffles is to insert expression (4.97) into Eqs. (4.96) and perform the sum over baffles, n, with the aid of the baffle spacings (3.24). The result, after approximating S by its value for $N = l'_n/l_n$ at those baffles which dominate the sum, is Eqs. (3.32a) and (3.33a). This result is discussed in Sec. III.E.2.

2b. Two Sets of Baffles

Having seen that coherent effects are not important in the case of a single set of baffles, we can be quite sure they also are not important when both ends of the vacuum pipe are baffled. This justifies our using the results of this report's intensity analyses to infer, from the one-set-of-baffles case, the noise for the two-sets-of-baffles case:

When two sets are present, diffraction of light off the first set will suppress the field arriving at the second set by the square root of expression (4.51), with the height-safety factor δH replaced by $\delta H_{\rm eff} = H$. Thus, the light coming into baffle n of the second set, after N reflections, will be given by

$$\psi_{\rm in} = \left(\frac{1}{32\pi^2} \frac{\lambda}{H} \frac{1}{\theta_{nN}} \right)^{1/2} \times [\text{Expression (4.79)}] \,. \tag{4.98}$$

As in the one-set-of-baffles case, the sum over N will be dominated by $N = l'_n/l_n$, which means $\theta_{nN} \simeq 2\theta'_n \simeq 2R/l_n$; and correspondingly, the net noise $\tilde{h}$ will be given by expressions (4.96) with

$$\sum_{N=1}^{\theta_* L/2R} (A_{nN}^{\rm diff})^2 + \sum_{N=l'_*/l_*}^{\theta_* L/2R} (A_{nN}^{\rm DAR})^2 \simeq \frac{1}{32\pi^2} \frac{\lambda}{H} \frac{l_n}{2R} \times [\text{Expression (4.97)}] \,. \tag{4.99}$$

By inserting (4.99) into (4.96), summing over baffles, and approximating the effects of the suppression factor S by its value at the baffles which dominate the sum, we obtain Eqs. (3.32b) and (3.33b) for the scattering noise. This noise is discussed in Sec. III.E.

Acknowledgments

For many helpful discussions I thank M. Burka, A. Cadez, P. Saulson, and R. Weiss.

References

[1] M. Stephens, measurements in support of the LIGO Project carried out at MIT in May 1987.

[2] J. M. Elson and J. S. Bennett, *Opt. Eng.*, 13, 116-124 (1979).

[3] A. Cadez, *Phys. Rev. XXX*, in press.

[4] M. Born and E. Wolf, *Principles of Optics*, Sixth Edition (Pergamon Press, Oxford, 1980).

[5] K. S. Thorne, in *300 Years of Gravitation*, eds. S. W. Hawking and W. Israel (Cambridge University Press, Cambridge, 1987).